

Contracts

ERRATA - 26 October 1965

The following correction is applicable to AFFDL-TR-65-136,
"Experimental Verification of the Analyses and Computer Programs
Concerning Heat Transfer Through Semitransparent Materials",
July 1965:

Add the following to the Foreword page:

Recommendations concerning changes or improvements to the
General American Transportation Corporation coated and uncoated
single glaze computer program which forms the subject of this
experimental verification program were reported by GATC in FDL-
TDR-64-39. These changes were not incorporated into the computer
program since GATC was not authorized to make such changes. The
reader is invited to compare the conclusions and recommendations
formed by GATC with those of Midwest Research Institute.

FOREWORD


The objective of the project was to experimentally evaluate the analyses and computer programs concerning heat transfer through semi-transparent materials which were developed under Contract No. AF 33(657)-9138. The work described in this report was conducted for the Air Force Flight Dynamics Laboratory, Research and Technology Division, under Contract No. AF 33(615)-1801 by the Midwest Research Institute, Kansas City, Missouri. The contract was initiated under Project No. 1368, "Structural Design Concepts", Task No. 136802, "Window System Concepts."

Lt. Michael Mann was the RTD project engineer for the first six months; Lt. Joseph Pharmer was the project engineer for the duration of the project. The work reported covers the period from April 1964 to June 1965.

Mr. Harold L. Finch, Project Leader, directed and worked on all phases of the project. Mr. Duncan Sommerville was responsible for the computer programming; Mr. Michael Noland conducted experimental tests and calibrated the equipment and specimens; and Mr. C. E. Moeller worked on the equipment design and the development of glass temperature sensors.

The manuscript was released by the authors June 1965 for publication as an RTD Technical Report.

Publication of this report does not constitute Air Force approval of the report's findings or conclusions. It is published only for the exchange and stimulation of ideas.



Holland B. Lowndes

HOLLAND B. LOWNDES
Acting Chief
Structures Division

ABSTRACT

An experimental and analytical evaluation of the theory and computer programs concerning heat transfer through semitransparent solids has been conducted by Midwest Research Institute (MRI). A transparent boundary apparatus was developed to experimentally evaluate the computer program developed under Contract AF 33(657)-9138 by the MRD Division of the General American Transportation Corporation (MRD). Experimental investigations of the heat transfer through 96 per cent silica glass and aluminosilicate glass were conducted for glaze temperatures to 1000°F. Similar data were produced for the same materials with tin oxide or gold films on one or both sides of the specimens.

The MRD computer program was modified to duplicate the experimental boundary conditions and facilitate use of the program. Computer runs were then conducted to insure that the original program and the modified program produced identical analytical results, i.e., that the modifications did not alter the basic theory or numerical techniques of the program. Since the modified program was written by MRI primarily for use in evaluating the MRD program, no attempt was made to document the modified program for general use.

Evaluation of the computer program was initiated by investigating over one hundred test conditions both in the laboratory and on the computer. Glaze thickness, glaze material, heat flux, surface temperature, film material, and film location were varied to produce a wide variety of conditions. Correlation between the MRD computer results and the experimental results was found to be unsatisfactory.

The experimental data were verified by numerous empirical and analytical tests. Several independent tests specifically designed to evaluate the computer program were then run; the findings of each of these investigations were in very close agreement and demonstrated that the program did not yield correct results. Significant errors in the computation of the "transparent" radiation interchange terms were found to be the source of the difficulties in the MRD computer program.

The experimental, empirical, and analytical tests conducted to evaluate the computer program led to the MRI conclusion that the program in its present form does not yield realistic results and thus is not a satisfactory tool for the computation of heat fluxes or temperature distributions in semitransparent materials.

Recommendations for further research are made based upon a belief that the theory is sound and that, despite the MRD computer program difficulties, the program can be made into an important tool for the design of advanced aerospace systems.

TABLE OF CONTENTS

	PAGE
I. INTRODUCTION	1
II. EXPERIMENTAL PROGRAM	3
A. COMPARISON OF TRANSPARENT AND OPAQUE TYPES OF APPARATUS .	3
B. DESIGN AND DEVELOPMENT OF APPARATUS, INSTRUMENTATION, AND FILMS	5
C. CALIBRATION OF APPARATUS	22
III. ANALYTICAL PROGRAM	30
A. THEORY OF HEAT TRANSFER THROUGH DIATHERMANOUS MATERIALS .	30
B. MRD COMPUTER PROGRAM	31
C. MODIFIED COMPUTER PROGRAM	35
D. COMPARISON OF THE MRD AND MODIFIED COMPUTER PROGRAMS . . .	38
IV. EVALUATION OF COMPUTER PROGRAM	41
A. EXPERIMENTAL TESTS	41
B. EMPIRICAL CALCULATIONS	41
C. COMPUTER PROGRAM RESULTS	44
D. PROGRAM EVALUATION	46
V. CONCLUSIONS AND RECOMMENDATIONS	51
APPENDIX A - PROPERTIES OF DIATHERMANOUS MATERIALS	55
APPENDIX B - DERIVATION OF THE LOCAL CONFIGURATION FACTOR FOR PARALLEL, DIRECTLY OPPOSED PLANE CIRCULAR DISKS	58
APPENDIX C - EXPERIMENTAL DATA	61
REFERENCES	73

LIST OF ILLUSTRATIONS

FIGURE	TITLE	PAGE
1	SCHEMATIC VIEW OF TRANSPARENT BOUNDARY APPARATUS	6
2	TRANSPARENT BOUNDARY APPARATUS SHOWING EDGE OF RADIANT HEATER, 3 GAS BURNERS, AND GLASS SPECIMEN WITH A PRELIMINARY PATTERN OF GOLD SURFACE TEMPERATURE SENSORS	7
3	RADIATION HEATER	8
4	EFFECT OF SOURCE TEMPERATURE ON TRANSMISSION OF THERMAL RADIATION THROUGH A THIN SHEET OF 96 PER CENT SILICA GLASS	10
5	SURFACE TEMPERATURE VARIATION OF RADIANT HEATER	11
6	SCHEMATIC OF WINDOW AND HEATER CONFIGURATION	12
7	CONFIGURATION FACTORS FOR TWO PARALLEL DISKS	13
8	STAINLESS STEEL "WINDOW" SURFACE TEMPERATURE DISTRIBUTION AND REPEATABILITY DATA FOR CONVECTIVE HEATING	16
9	96 PER CENT SILICA SPECIMEN WITH TWO GOLD TEMPERATURE SENSORS ON EACH SIDE	17
10	SCHEMATIC OF APPARATUS COMPONENTS, INSTRUMENTS AND CONTROLS . .	19
11	INSTRUMENT AND CONTROLS CONSOLE USED WITH TRANSPARENT BOUNDARY APPARATUS	19
12	ALUMINOSILICATE SPECIMEN COATED ON THE BACK SURFACE WITH A 0.2 μ FILM OF GOLD	20
13	SPECTRAL TRANSMITTANCE OF A 0.2- μ GOLD FILM COATED ON ONE SURFACE OF A THIN SHEET OF GLASS	21
14	CALIBRATION OF RADIANT HEATER THERMOCOUPLE USING AN OPTICAL PYROMETER	23
15	CALORIMETER FLOW RATE DATA FOR A CONSTANT HEAT FLUX	25
16	CALORIMETER CALIBRATION	26

LIST OF ILLUSTRATIONS (Continued)

FIGURE	TITLE	PAGE
17	THERMAL CONDUCTIVITY OF TYPE 304 STAINLESS STEEL AS DETERMINED BY TRANSPARENT BOUNDARY APPARATUS	27
18	TYPICAL CALIBRATION CURVES FOR WINDOW SURFACE TEMPERATURE SENSORS	29
19	WINDOW CROSS SECTION	33
20	INFLUENCE OF NUMBER OF WAVELENGTH BANDS ON PROGRAM ACCURACY . .	37
21	OUTPUT DATA BEFORE (a) AND AFTER (b) CORRECTING FAULTY TEST . .	40
22	EFFECTIVE EMISSIVITY OF SODA LIME GLASS AS DETERMINED BY GARDON	43
23	EXPERIMENTAL TEMPERATURE GRADIENT DATA	45
24	COMPARISON OF ANALYTICAL, EMPIRICAL AND EXPERIMENTAL DATA . . .	45
25	COMPARISON OF EXPERIMENTAL AND ANALYTICAL TRANSIENT RESULTS . .	49
26	FIRST ORDER APPROXIMATION OF REFLECTANCE OF A THIN GOLD FILM .	49
C-1	EXPERIMENTAL DATA FOR 5/16 IN. 96 PER CENT SILICA GLASS	62
C-2	EXPERIMENTAL DATA FOR 1/4 IN. 96 PER CENT SILICA GLASS HEATED BY CONVECTION	63
C-3	EXPERIMENTAL DATA FOR 1/4 IN. 96 PER CENT SILICA GLASS	64
C-4	EXPERIMENTAL DATA FOR 1/8 IN. 96 PER CENT SILICA GLASS	65
C-5	EXPERIMENTAL DATA FOR 1/8 IN. 96 PER CENT SILICA GLASS	66
C-6	EXPERIMENTAL DATA FOR 1/4 IN. ALUMINOSILICATE GLASS HEATED BY CONVECTION	67
C-7	EXPERIMENTAL DATA FOR 1/4 IN. ALUMINOSILICATE GLASS COATED WITH 0.2 μ TIN OXIDE FILMS ON BOTH SURFACES	68

LIST OF ILLUSTRATIONS (Concluded)

FIGURE	TITLE	PAGE
C-8	EXPERIMENTAL DATA FOR 1/4 IN. ALUMINOSILICATE GLASS COATED WITH A 0.2 μ TIN OXIDE FILM ON THE HOT SURFACE	69
C-9	EXPERIMENTAL DATA FOR 1/4 IN. ALUMINOSILICATE GLASS COATED WITH A 0.2 μ TIN OXIDE FILM ON THE COLD SURFACE	70
C-10	EXPERIMENTAL DATA FOR 1/4 IN. ALUMINOSILICATE GLASS COATED WITH 0.2 μ GOLD FILMS ON BOTH SURFACES	71
C-11	EXPERIMENTAL DATA FOR 1/4 IN. ALUMINOSILICATE GLASS COATED WITH A 0.2 μ GOLD FILM ON THE COLD SURFACE	72

NOMENCLATURE

A	- Area
E	- Emissive power.
F_A	- Local configuration factor from window to heater.
F_E	- Factor accounting for departure of window and heater from complete blackness.
$f(\epsilon)$	- Function relating apparent emissivity to thickness and temperature.
h	- Distance from window upper surface to heater; see Figure 6.
K	- Thermal conductivity.
L	- Glaze thickness.
n	- Index of refraction.
P	- Auxiliary function.
\hat{P}	- Defined by Eq. (23).
P'	- Defined by Eqs. (31) and (32).
p	- Fraction of blackbody energy
$Q_A(x_i)$	- Flux absorbed at x_i from external radiation source.
$Q_R(x_i)$	- Flux reabsorbed at x_i from the other elements.
q	- Heat flux.
q_{net}	- Heat flow into calorimeter.
q_i'''	- Net radiant interchange at x_i .
q''	- Convective heat flux.
R	- Electrical resistance.
R_H	- Heater radius.
R_W	- Window radius.

Contrails

r_H	- Variable radius of heater.
r_W	- Variable radius of window.
S	- Constant.
T	- Temperature.
T_{in}	- Calorimeter water inlet temperature.
T_{out}	- Calorimeter water outlet temperature.
v, V	- Electromotive force.
W	- Radiant flux.
\dot{w}	- Calorimeter water flow.
x	- Position coordinate.
y	- Auxiliary position coordinate.
α	- Angle between direction of beam within plate and normal to plate.
γ	- Absorption coefficient.
ϵ	- Emissivity.
λ	- Wavelength.
ρC	- Volumetric specific heat.
ρ	- Reflectance.
ρ'	- Directional reflectivity.
σ	- Boltzmann's constant.
τ	- Transmittance.
τ'	- Directional transmissivity.
ϕ	- Defined by Eq. (22).

Subscripts

B	- Burner.
C	- Calorimeter.
Cr	- Critical.
g	- Gas.
H	- External radiation source (heater).
i,j	- Elements.
m	- Wavelength band.
R	- Environment (room).
T	- Transparent.
W	- Window.
λ	- Wavelength.
1	- First element, hot surface.
11	- Eleventh element, cold surface.
\perp	- Perpendicular polarization.
	- Parallel polarization.

I. INTRODUCTION

Heat transfer is an important consideration in the development of advanced aerospace systems. Although methods employed by vehicle designers to determine heat flow through opaque solids are time-proven, techniques for the thermal analysis of heat transfer in semitransparent* materials are not well established. Such methods are needed to design the semitransparent window systems of hypersonic and re-entry vehicles.

Theoretical methods of describing heat transfer by phonon (lattice) conduction in semitransparent solids have been developed in recent years (Refs. 1 and 2). These techniques give realistic results when used to analyze glazes at low temperatures, but at high temperatures the results do not correlate well with experimental data. Gardon (Ref. 3) and other investigators advance the theory that at elevated temperatures a significant amount of heat flows through nonopaque solids by photon (radiative) conduction.** In contrast with opaque materials, absorption and emission take place internally as well as at the surfaces. The degree of photon conduction is a function of the solid's thickness and temperature (Ref. 4).

Gardon has developed a theoretical method of analyzing thermal energy propagation by the combined mechanisms of phonon and photon conduction. An operational computer program based on his theory has been written by the MRD Division of the General American Transportation Corporation (MRD) for an IBM 7094 computer; however, the theory as well as the program must be verified before it can be used with confidence.

Midwest Research Institute (MRI) was contracted to experimentally evaluate the computer program for glaze temperatures to 1000 F. A unique feature of the apparatus developed for the evaluation was that the window surfaces had a transparent boundary, whereas in most studies of heat transfer in glass, one or both of the surfaces are in contact with an opaque material. Thus the tests were carried out under conditions similar to those encountered in actual vehicle flights. The choice of a transparent-boundary apparatus is supported by Lee (Ref. 2) who states that "for highly transparent materials the 'effective' conductivity (phonon plus photon conductivity) measured is largely determined by boundary conditions unless extremely thick specimens are used."

* Semitransparent includes materials generally considered to be transparent (e.g., glass).

** Photon conduction is so called because of the analogy between this mechanism and the familiar lattice thermal conduction.

The development and calibration of the apparatus is described in Section II of this report. Gardon's theory, the MRD computer program, and a modification of the program are summarized in Section III. Modifications include temporary changes required to give better agreement with the experimental program, to evaluate the program's accuracy, and to facilitate the preparation of data. The evaluation tests, data, and analysis of results are described in Section IV. Conclusions and recommendations for improving and applying the program are given in Section V.

Derivations, other supporting information and the experimental data are included in the Appendices.

II. EXPERIMENTAL PROGRAM

Evaluation of the computer program is fundamentally an experimental problem. Before designing an apparatus to simulate radiative and/or convective heat transfer through aerospace windows, a survey was made of previous experimental studies of glass. These investigations, which were primarily concerned with making effective thermal conductivity measurements, in general had one similarity: the glass specimens were bounded on one or both surfaces by opaque materials, usually metal foils.

Preliminary plans for an apparatus having transparent boundaries were developed. A comparison of the two types of apparatus, herein designated as Transparent-Boundary Apparatus (TBA) and Opaque-Boundary Apparatus (OBA), is given below.

A. Comparison of Transparent and Opaque Types of Apparatus

The major differences of the TBA and OBA are the manner heat is supplied to the specimen, the surface temperature determinations, and the heat flux measurements.

Heat source: The source of heat which is transmitted through the TBA specimen is from virtually transparent hot gases (convection) and/or a radiation heater (radiation). Generally, heat is transmitted through an OBA specimen by conduction from a metal foil in physical contact with the hot side of the specimen and by the net radiation interchange between foils at the hot and cold sides. Thus, the influence of external radiant energy on the specimen can be directly determined with TBA, indirectly by OBA (by using pairs of foils with various emissivities)(Ref. 5).

Surface temperature determinations: The surface temperature determinations are made by using sensors applied directly on each side of the TBA specimen. These sensors are small resistance grids. Hence, the surface temperatures are directly measured. The temperatures of the OBA specimen are measured by thermocouples installed in a metal bar behind the foil on each side of the specimen. The surface temperatures are then determined by extrapolating data of specimens of several thicknesses (to correct for thermal contact resistance). In recent work at NBS, the temperature gradient through the specimen was measured by thermocouples cemented in grooves in the edge of the specimen (Ref. 5).

Heat measurement: The rate of heat transmission through the TBA specimen is measured by a water calorimeter (the central part of the heat sink). The rate of heat transmission through the OBA specimen is determined by measuring the electrical power supplied to the specimen heater and correcting for heat not passing through the specimen.

After weighing the relative merits of the two basic types of apparatus, it was concluded that the OBA should not be used. Some of the objections to the use of opaque boundaries were:

1. The environmental conditions would not realistically simulate those encountered in actual aerospace vehicle flights;
2. Internally generated radiation would be reflected or absorbed by the foils;
3. The glass surfaces having opaque boundaries would not emit heat to space;
4. The unrealistic boundary conditions would largely determine the net heat flow for relatively thin specimens comparable to those used in aircraft window systems (Ref. 2); and
5. The temperature of the external radiative "heater" (the foil) could not be made independent of the specimen temperature.

To illustrate one of the difficulties associated with opaque boundaries, an amplification of the fifth objection follows. Assume that a window is to be heated to a steady-state temperature of 500 F. The "radiator" temperature will also be 500 F since the foil, which represents the heater, must be in intimate contact with the window surface to minimize thermal resistance.

Most glasses are transparent to some of the energy that radiates between 0.5μ and 4.5μ . Within this band impinging radiation is partially absorbed, partially reflected, and partially transmitted. Outside of this band radiation is reflected or absorbed. At 500 F, less than 20 per cent* of the emissive power of the heater will be at wavelengths to which glass is transparent and only a fraction of this amount will be transmitted through the window. Thus, at moderate glass temperatures the ratio of external radiative

* In actual flight, up to 99 per cent (depending on the heat source) of impinging radiation is within the transparent spectrum of glass.

conduction to phonon conduction is very low and consequently the opaque boundary method cannot adequately evaluate the portion of the program that pertains to external radiation. At elevated glass temperatures, radiation from the foil is no longer insignificant; nevertheless verification of the program is still limited to the single hypothetical case where the heater and glass surface temperatures are the same.

A further difficulty associated with opaque boundaries is that this method does not permit direct evaluation of the program for the case where there is no external radiation, that is, for the case where convection is the only means of transmitting heat to the window.

B. Design and Development of Apparatus, Instrumentation, and Films

Since opaque boundaries would prevent a satisfactory evaluation of the subject computer program, an apparatus with transparent window boundaries was designed and built. The final assembly and components are illustrated in Figures 1 and 2.

The heat source consisted of two types of heat generating systems: high velocity gas burners and an electric radiant heater. These were located and controlled so that they could be used simultaneously or individually without restricting the operation of the other. The specimen was a disk 4 in. in diameter and 1/8 in., 1/4 in., or 5/16 in. thick. The surface temperatures of the specimen were sensed by gold resistance grids.

The specimen was supported 0.175 in. above a water cooled back plate. Heat was transferred across the gap by radiation and conduction through the air; forced convection was not required. The heat sink was water cooled and coated with a "black" paint to minimize the amount of heat emitted or reflected back to the specimen. The central portion of the water cooled plate was a calorimeter or thermopile.

The apparatus components, temperature sensors, and instrumentation are described in detail below.

Radiation heater: The radiative heater was designed to satisfy three fundamental requirements:

1. That the heat flux be emitted at wavelengths that generally coincide with the transparent band of glass;

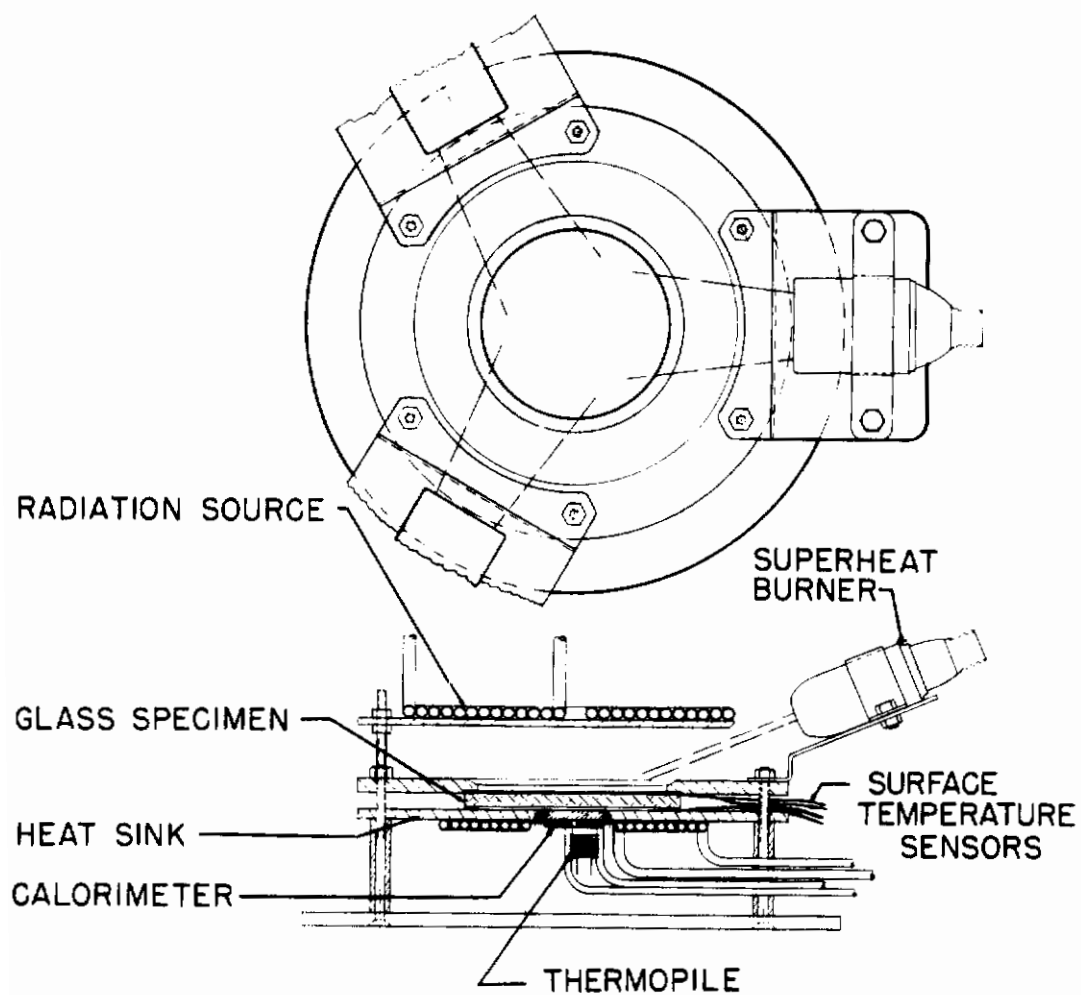


Figure 1 - Schematic View of Transparent Boundary Apparatus

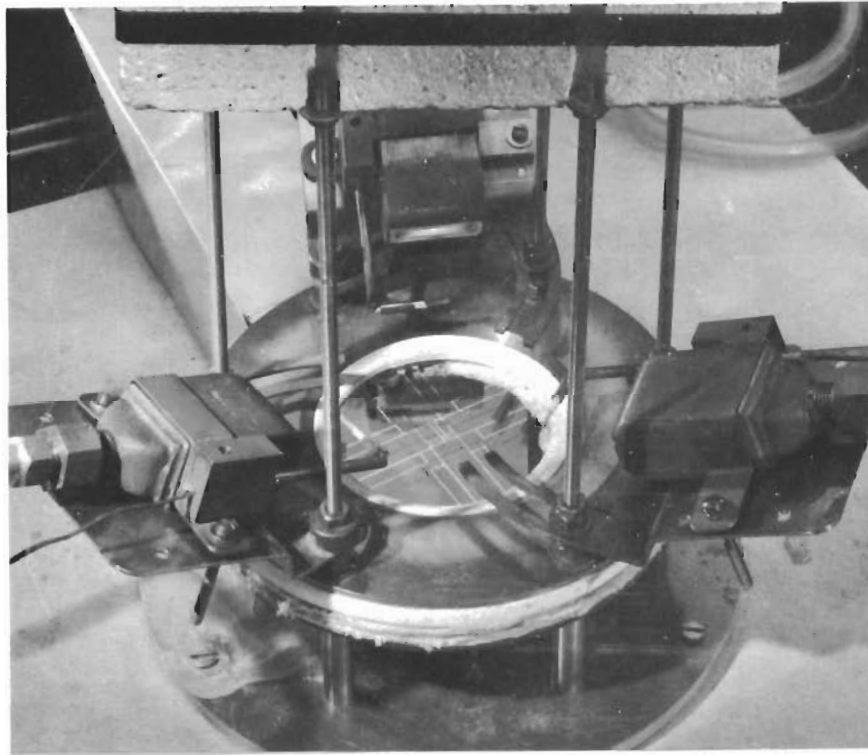


Figure 2 - Transparent Boundary Apparatus Showing Edge of Radiant Heater, 3 Gas Burners, and Glass Specimen With a Preliminary Pattern of Gold Surface Temperature Sensors

2. That the heat flux be uniformly distributed over the window surface; and

3. That the magnitude of impinging heat flux be sufficient to heat diathermous materials to 1000 F.

Several types of heaters were fabricated and evaluated. The first design consisted of a 0.032 in. Kanthal wire and a ceramic disk. The heating element was imbedded and cemented with aluminum oxide in a groove which formed a spiral in the ceramic plate. It was found that this heater could not be operated for any length of time at elevated temperatures (1800 - 1900 F); however, experimentation with coils of heavier gage Kanthal wire resulted in a unit that gave reasonable life at these temperatures.

The heater design ultimately adapted for the program is shown in Figure 3.



Figure 3 - Radiation Heater

It had an indefinite lifetime and its surface temperature was more uniform than the previous types. The heater had a spiral resistance element $\frac{3}{8}$ in. wide and $\frac{1}{16}$ in. thick with a resistance of approximately 0.1 ohm; maximum voltage was 20 v. It was made of Hastelloy X alloy, which has an adherent oxide coating at temperatures exceeding 2000 F and has sufficient strength at these temperatures to maintain its shape without sagging. To assure no distortion of the long spiral element, Hastelloy X rods ($\frac{3}{32}$ in. diameter) were butt welded to the flat spiral strip to provide support. These rods and the terminal rods passed through a refractory insulating block, 2- $\frac{1}{2}$ in. thick, and were held on the back of the block by clips. Thus the refractory block supported the heater element and thermally insulated the rear side of it. Two chromel-alumel thermocouples were clamped between the element and the insulation block, one for automatic control and the other for monitoring the heater temperature.

The primary purpose of the experimental tests was to evaluate the theory that predicts heat transfer through materials by the mechanism of radiation as well as by conduction. It was therefore essential that the radiative heater emit energy at wavelengths to which glass is transparent. Since the amount of transmission through the glass required to satisfy this criterion cannot be clearly defined, a conservative range of 10 - 50 per cent of incident radiation was arbitrarily established.

Most glasses are transparent to some of the energy that radiates between 0.5μ and 4.5μ . Planck's quantum theory was used to determine the heater temperature range that radiates predominantly within this range.

The amount of heat that is emitted within a given wavelength band is

$$q = E \int_{\lambda_1}^{\lambda_2} \frac{E_{\lambda}}{\sigma T^5} d(\lambda T) \quad (1)$$

where the emissive power is

$$E = \sigma T^4 \quad (2)$$

The functions $E_{\lambda}/\sigma T^5$ and λT are directly proportional and are presented in tabular form by Kreith (Ref. 6). It follows that the per cent of impinging radiation that is transmitted through a diathermanous material is

$$P = \int_0^{\infty} \frac{T_{\lambda} E_{\lambda}}{\sigma T^5} d(\lambda T) \quad (3)$$

Equation (3) was evaluated for a thin sheet of 96 per cent silica glass and the results are presented graphically in Figure 4. The curve indicates that the glass will transmit from 0 to 79 per cent of the incident energy and that maximum transmission is affected by a heater temperature of 6000 F. Further examination of Figure 4 reveals that the desired 10 - 50 per cent transmission range can be attained provided

$$900 \text{ F} \lesssim T_H \lesssim 2300 \text{ F} \quad (4)$$

A similar analysis with respect to aluminosilicate, borosilicate, soda lime, and fused silica glasses resulted in the same approximate heater temperature range in each case.

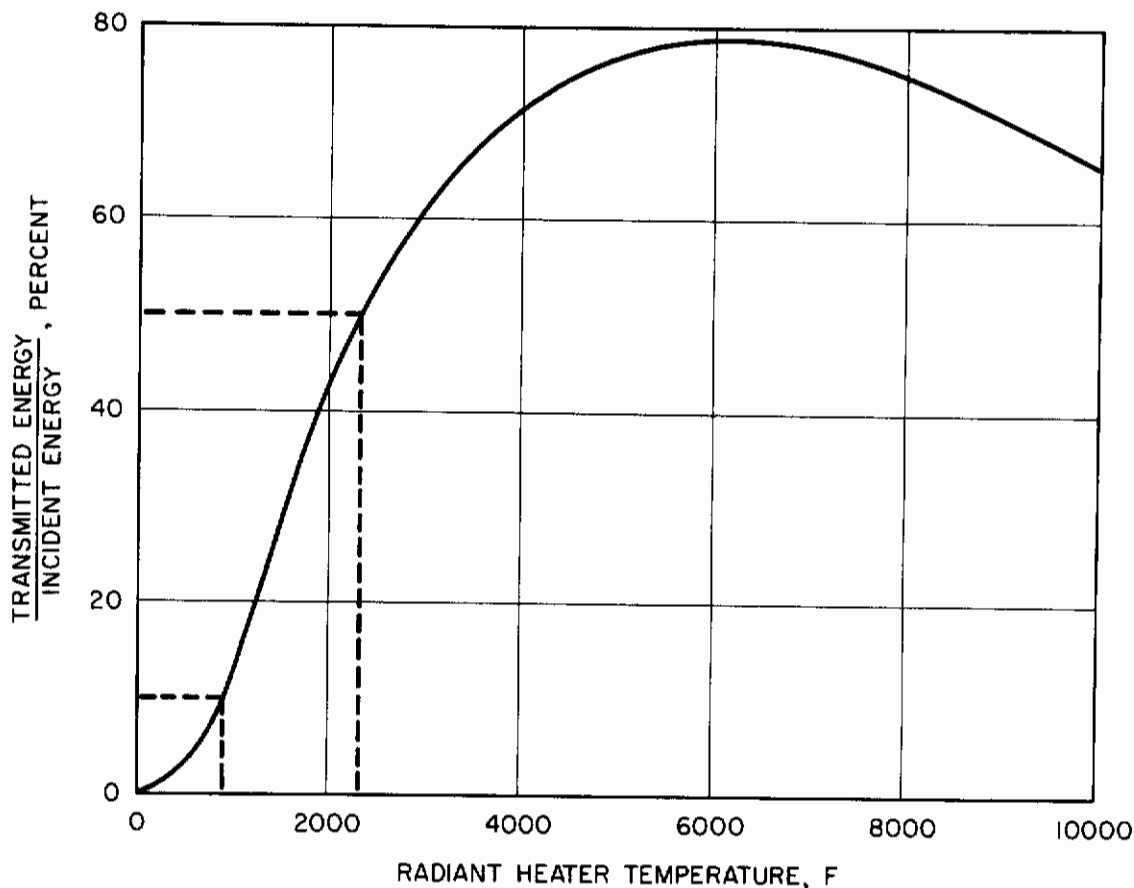


Figure 4 - Effect of Source Temperature on Transmission of Thermal Radiation Through a Thin Sheet of 96 Per Cent Silica Glass

The heat flow through aerospace windows in actual flight and in simulated flights on the subject computer program is essentially one-dimensional. Therefore in the experimental program it was important that the impinging radiation be uniformly distributed over the window surface. This can be accomplished with a disk-shaped heater provided its surface temperature, T_H , is uniform and the relative size and the spacing of the heater and window are carefully analyzed.

The temperature distribution of the heater was determined with an Ircon model 300 optical pyrometer. The results, which are illustrated in Figure 5 indicate that at $T_H \approx 1150$ F the absolute temperature varied by ± 1 per cent, and at $T_H \approx 1650$ F the absolute temperature varied by ± 2 per cent. These differences result in maximum variations of emissive power of approximately 4 and 8 per cent, respectively.

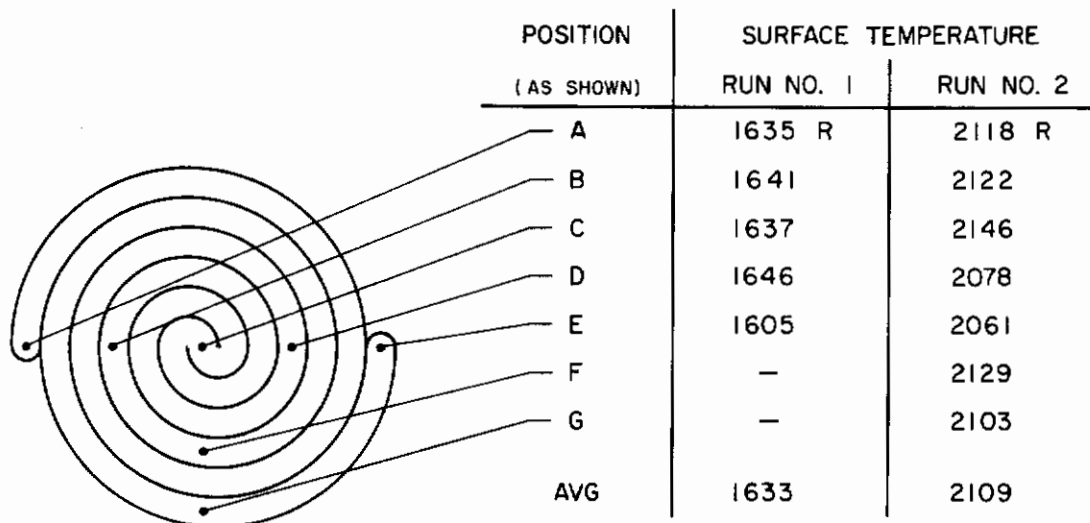


Figure 5 - Surface Temperature Variation of Radiant Heater

If the heat is emitted uniformly it will impinge the window uniformly provided either of the following conditions exists:

1. The heater is designed and positioned in such a way that every element on the window surface "sees" nothing but the heater; or
2. The heater is positioned such that it is "seen" equally well by each element of the window surface.

The first criterion is satisfied if $r_H/r_W \rightarrow \infty$ or $h \rightarrow 0$; the second requires that $h \rightarrow \infty$. The variables r_H , r_W and h are illustrated in Figure 6. These ideal conditions are not practical in the laboratory; therefore, reasonable compromises based on further analysis were made.

The local heat flux impinging the window surface is

$$q = \sigma F_A F_E (T_H^4 - T_W^4) \quad (5)$$

where F_A is the local configuration factor which allows for the average angle through which the heater is "seen," F_E makes allowance for the departure of the source and receiver from complete blackness and is a function of their individual emissivities. Equation (5) and the corresponding theory was developed by Hottel. This widely used approach is described in detail in McAdams' classic heat transfer text (Ref. 7).

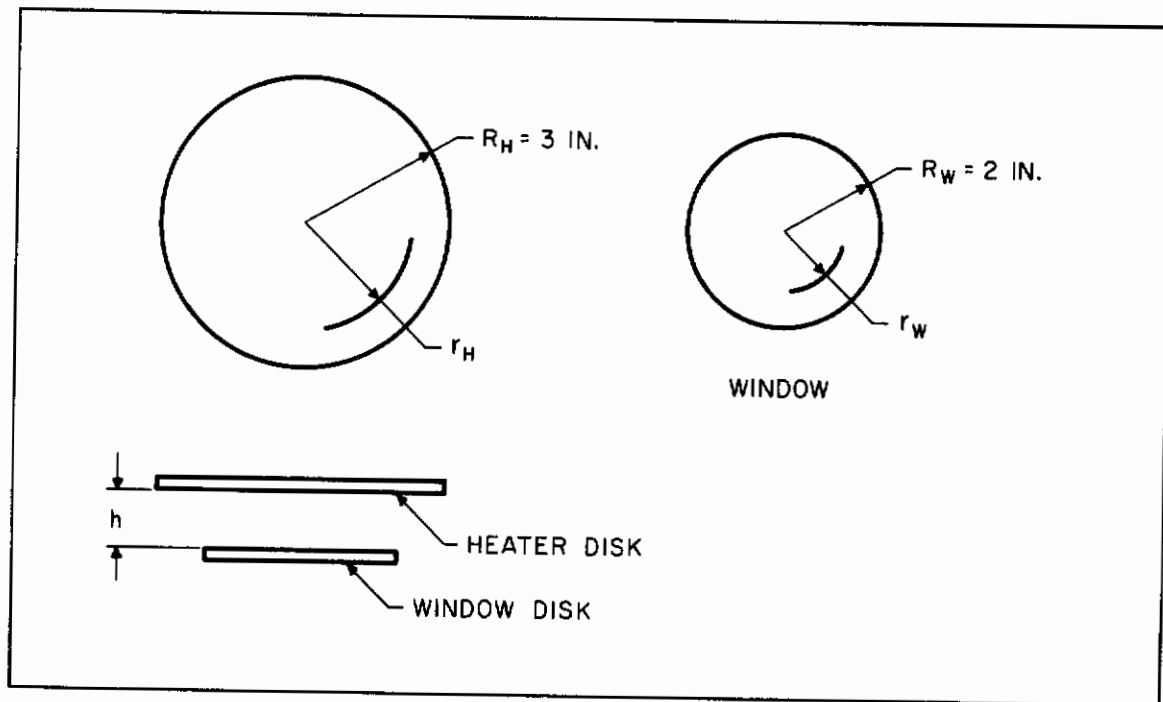


Figure 6 - Schematic of Window and Heater Configuration

The shape factor frequently reported and used for two parallel, finite disks is an average value and does not account for local variations. Since it is these variations that must be minimized in the experimental program, the apparatus design cannot be based solely on standard gray-body theory as set forth by Hottel or Eckert and Drake (Ref. 8). However, their approach can be extended to be applicable to the heater design analysis by employing shape factor algebra - that is, by subdividing the disks into rings and using the modified reciprocity relationships described by Kreith (Ref. 9). A study to determine the relationship between the local configuration factor and the variables h and r_W for $R_H = 3$ was made (see Figure 6). The theoretical approach and sample calculations are presented in Appendix B and the results are plotted in Figure 7. For comparison, the average values of F_A were obtained from configuration charts developed by Hamilton and Morgan (Ref. 10) and are plotted as dashed lines for $h = 2.0 \text{ in.}$ and $h = 4.0 \text{ in.}$

The configuration factor curves indicate that the per cent deviation of the local value of F_A from the average is greatest when the heater is positioned about 3 in. from the window. At $h = 2.0$ and $h = 4.0$ the variation from average is approximately ± 15 and ± 10 per cent, respectively. As expected, F_A approaches a constant as $h \rightarrow 0$ or when $h \gg 1$. At $h = 0.4 \text{ in.}$, F_A deviates from the average by less than 2 per cent; at $h = 8.0 \text{ in.}$, the variation is approximately 4 per cent. Primarily as a result of this analysis, the following heater positions were selected for the experimental program:

$$h = 9/16 \text{ in. and } h = 8 \text{ in.} \quad (6)$$

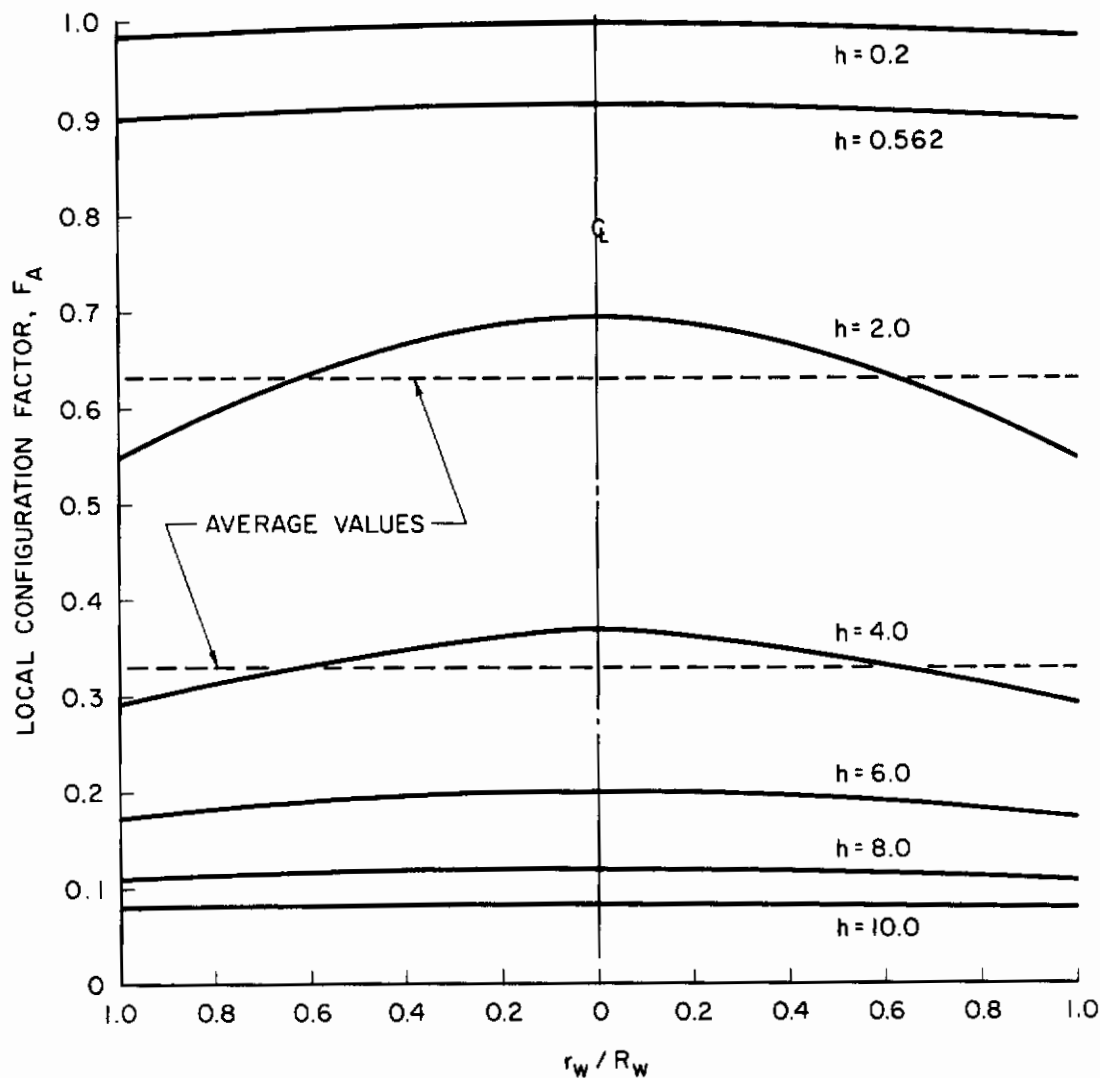


Figure 7 - Configuration Factors for Two Parallel Disks

A study was made to determine the heater temperatures required to raise the temperature of a glass window to 1000 F or above. Heat was considered to be transferred through the window by conduction only; however, compensation for this assumption was made by employing apparent emissivities and thermal conductivities (see Section IV-B). The results of the analysis indicated that the surface of the window closest to the heater would stabilize at approximately 1100 F when $T_H = 1300$ F and $h = 9/16$ in. This conclusion was subsequently verified experimentally.

It was concluded that a radiant heater could be designed, positioned, and operated to satisfy all three of the fundamental requirements set forth at the beginning of this section. Based on analyses described above, two heater

position/temperature combinations were used throughout the experimental program. For the case where radiation was the primary source of heat transfer to the window, the heater was positioned 9/16 in. above the glass and operated at temperatures between 900 and 1300 F. For the case where radiation and convection were simultaneously used, the heater was placed 8 in. above the window and operated at temperatures up to 2300 F. The heater was also used in this position without operating the burners.

Convection heaters: The convective heat source was designed to satisfy two fundamental requirements:

1. That the convective heat transfer be sufficient to heat diathermanous materials to 1000 F; and
2. That the heat flux be uniformly distributed over the window surface.

Preliminary calculations were made to determine the mean gas temperature necessary to heat the exposed glass surface to 1000 F. Using a conservative convective heat transfer coefficient (for parallel gas flow) and effective thermal conductivity and emissivity values for glass, a maximum gas temperature of 2880 F was computed. Based on this estimate, a superheat burner supplied with natural gas and compressed air was selected as the convective source.

The burner used in the experimental program was a SH-2 Selas superheat burner with a rectangular blast opening 1-3/8 in. long by 1/8 in. wide and a flared tongue. Combustion occurs inside the burner and the products of combustion are forced out of the blast opening at a high velocity. When the burner is first ignited, the flames burn outside of the combustion chamber and must be forced or "popped" back into the burner. A technique of accomplishing this with a torch directed into the combustion chamber was developed.

The convective source consisted of three burners mounted so that they could each be adjusted in three directions (see Figure 2). Various combinations of burner positions were experimentally evaluated to determine the optimum arrangement with respect to uniform heating. These tests were run on a 1/32 in. stainless steel "window;" the temperature distribution was determined by thermocouples welded to the backside at 12 different positions.

Initially, the burners were directed towards the center of the stainless steel disk as schematically shown in Figure 1. Uneven heating was indicated both by a nonuniform oxidation pattern and by a measured temperature gradient of several hundred degrees. These results are in general agreement with those of Gardon who studied local heat transfer between three exhausts of hot air and

a plate mounted perpendicular to them (Ref. 11). The MRI burners were then lined up tangentially to the specimen's periphery and the result was a markedly improved heat distribution. By systematically varying the fuel flow rates, heater positions, and other pertinent variables, it was found that temperatures over the central two-thirds of the "window" could be made uniform within ± 2 per cent of the absolute temperature. The maximum variation of ± 25 F is comparable to that attained with the radiative heater operating at a height of 9/16 in. and therefore the variations in heat flux rate should also be comparable and satisfactory.

Unlike the radiative case, it is not a simple matter to obtain repeatable magnitudes of heat flux from test to test. For convective heating, the air flow rate and the exhaust temperature must be controlled for each of the three burners. The exhaust temperatures were indicated by thermocouples positioned in front of the burners (see Figure 2) and were varied by manually adjusting the gas flow rate. Despite double pressure regulators, which were used in both the air and natural gas supply lines, the burner temperatures fluctuated over a range of ± 25 F at 2000 F. However, the average temperature of each burner was monitored and the results were repeatable from one test to another for a given set of conditions.

The uniformity of convective heat distribution and the repeatability of heat flux rates are illustrated in Figure 8, which shows the temperature profile of a 1/32 in. stainless steel disk for two similar runs made at a time interval of 20 days.

Temperature sensors: The temperature sensor developed for measuring the surface temperatures of the specimen was a gold resistance thermo-element. Fine wire platinum-platinum 10 per cent rhodium thermocouples were originally considered but were abandoned because of the difficulty of attaching them to the surface without disturbing the heat transfer to the surface and because of their low sensitivity.

Gold was adopted for the resistance grid of the temperature sensor because the metal has a high thermal coefficient of resistivity, is free from oxidation, is stable for temperatures to at least 1200 F and is readily deposited with reproducible resistance. Two gold grids were deposited on each side of the specimen as shown in Figure 9. The top and bottom grids were deposited directly opposite each other so that local surface temperature gradients are cancelled out. The grids consisted of two main current conductors and two voltage taps; the latter were used so that the resistance change of the grid in the center of the specimen surface could be determined. The "active" section of the grid was "U" shaped, 1-1/2 in. long, and 0.005 to 0.006 in. wide. The resistance of this section was within the range of 5 to 10 ohms at 77 F; it had a temperature coefficient of resistivity of approximately 0.020 ohm/F.

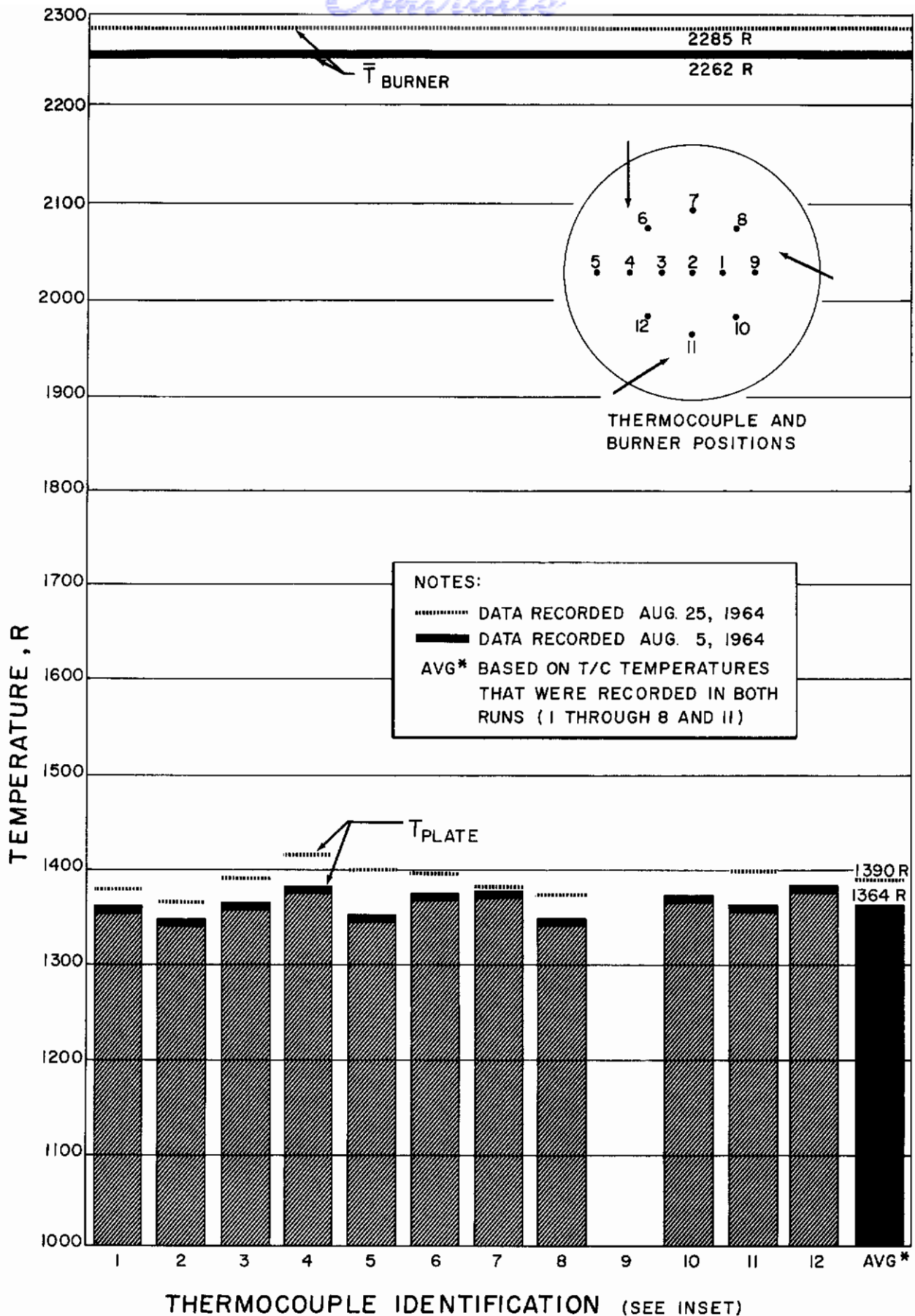


Figure 8 - Stainless Steel "Window" Surface Temperature Distribution and Repeatability Data for Convective Heating

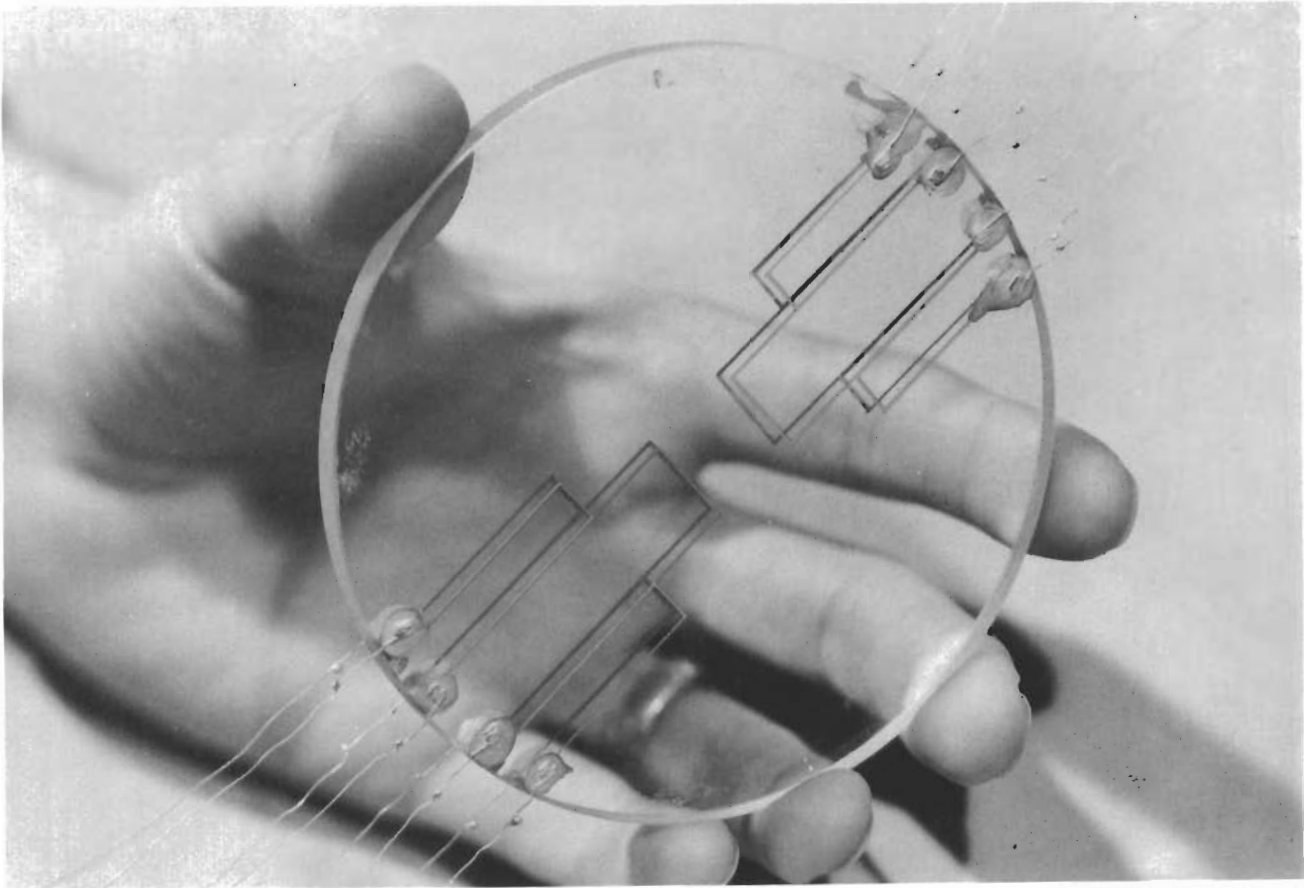


Figure 9 - 96 Per Cent Silica Specimen With Two Gold Temperature Sensors on Each Side

The gold was deposited onto the surface of the specimen by vacuum evaporation. Initially, the specimen was cleaned with a detergent, rinsed with distilled water, and flushed with reagent grade acetone. After the specimen was placed on a mask and installed in a vacuum chamber, a pressure of approximately 1×10^{-5} torr was obtained. The specimen was heated to between 950 and 1150 F for final surface cleaning. Then, a gold wire, 99.9 per cent pure, was heated in a molybdenum boat until it melted and evaporated to form a sufficiently thick film on the specimen. The thickness of the film was monitored during deposition by a resistance measuring circuit on a dummy specimen. When the resistance decreased to a standard value, the evaporation was stopped. Thus, grids could be produced with nearly identical resistances. When the specimen was cooled, the chamber was opened and the specimen moved to a new position over the mask and the procedure repeated.

Silver wires were used at the edge of the specimen to connect the grids to silver electrical conductors. These wires were bonded to the gold film of the grids with Wesgo No. F1406B silver brazing paint, fired in a furnace at 1100 F.

Heat sink and calorimeter: The heat sink for the apparatus was a water-cooled copper plate and a calorimeter, which was mounted at the center of the plate. The surfaces were flush with each other and were coated with a black paint having an emissivity of approximately 0.98. The specimen was supported so that it was 0.175 ± 0.010 in. above the heat sink. The space around the specimen between the heat sink and the specimen clamp was filled with alumina silicate fiber paper. Thus, the edges of the specimen were insulated from radial heat losses.

The calorimeter consisted of a copper disk of 1 sq. in. area with a copper cooling coil soldered to its bottom side. The copper disk was supported and insulated from the remainder of the heat sink by a nylon circular spacer. The temperature difference between the incoming and outgoing water was sensed by a five-junction chromel-constantan thermopile, made of wires 0.003 in. diameter. The wires were sealed in the copper tubing by epoxy cement. At the operating temperature of the calorimeter, the sensitivity of the thermopile was 0.1645 mv/F.

Instrumentation: The instrumentation and controls used with the apparatus are shown schematically in Figure 10 and are illustrated in Figure 11. The signals from the temperature sensors and the thermopile were measured with a L & N K3 potentiometer with a L & N linear D.C. amplifier as a null detector. The signals could be recorded with the K3 as a voltage suppression unit; the sensitivity of the recorder could be varied by the amplifier from 50 to 2,000 microvolts full scale.

The controlling system for the radiant heater consisted of a L & N electronic null detector, zener-diode stabilized voltage reference, L & N C.A.T. proportional controller, magnetic amplifier and a saturable core reactor. This system maintained the radiant heater temperature constant to within ± 0.4 per cent.

Thin films: The specimens used in the final phase of the experimental program were aluminosilicate disks coated with 0.2μ gold or tin oxide films. Four gold temperature sensing grids were deposited on each of the disks as previously described. A film was then vacuum deposited over the entire center section of one or both sides of the substrate; a fixture for supporting the disk also served as a mask to prevent the film from depositing on the terminals of the temperature sensors. In the case of gold films, fine diagonal lines were scribed through the coatings to prevent the resistance grids from shorting out.

A coated specimen is shown in Figure 12. The gold film, which is on the back side of the disk, has a mottled appearance as a result of being

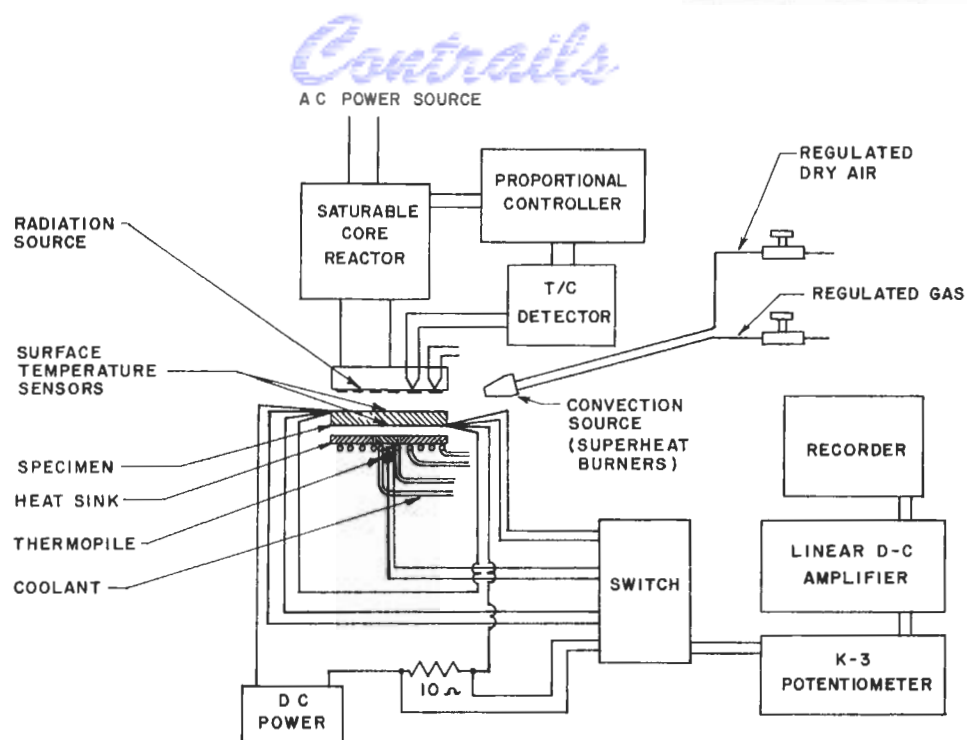


Figure 10 - Schematic of Apparatus Components, Instruments and Controls



Figure 11 - Instrument and Controls Console Used With Transparent Boundary Apparatus

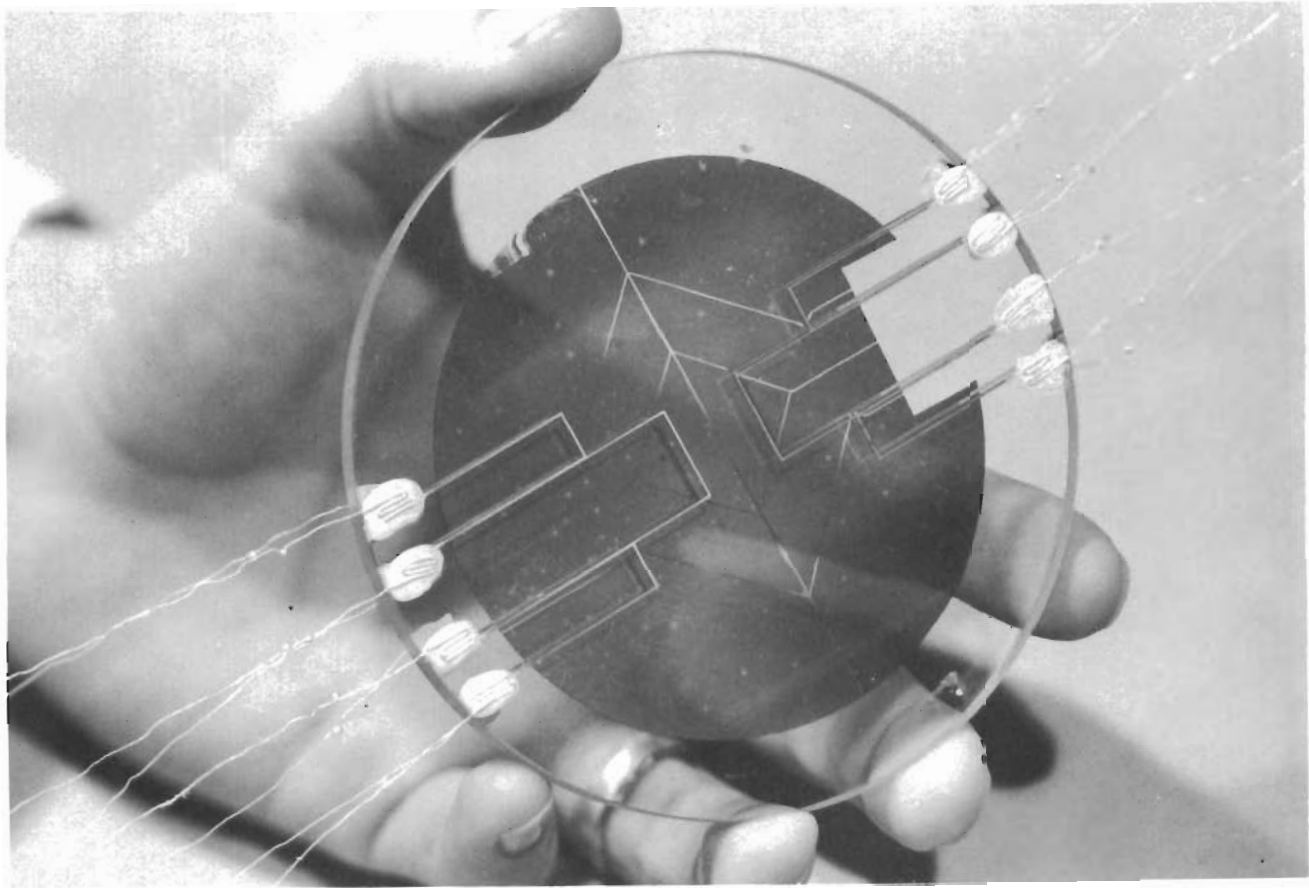
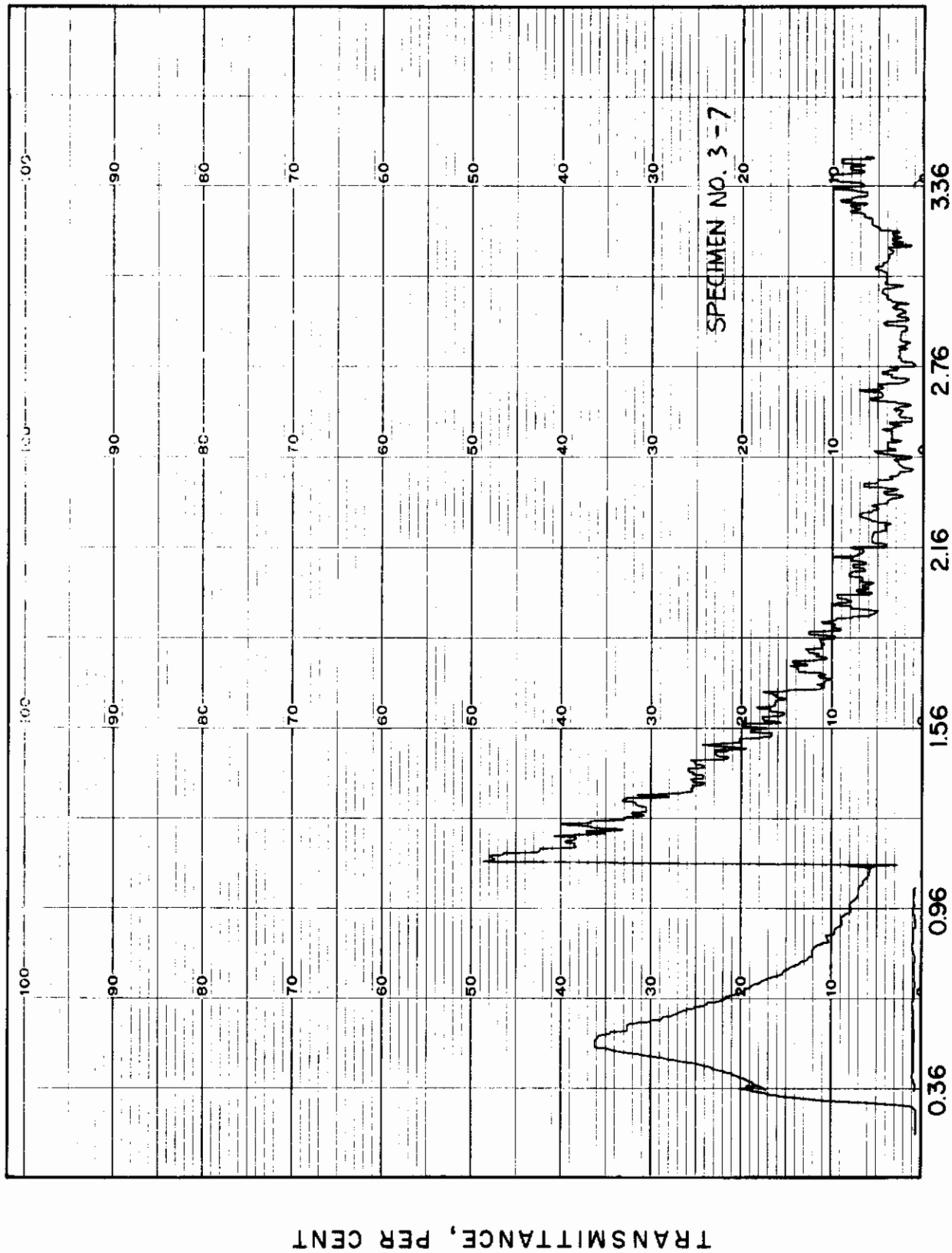


Figure 12 - Aluminosilicate Specimen Coated on the Back Surface
With a 0.2μ Film of Gold

aged for 24 hr. at 1100 F and being impinged by flames from the superheater burners for long periods of time. The transparency of the 0.2μ gold coating can be noted by observing the outline of the hand and fingers behind the film.

The notch in the upper right quadrant of the film shown in Figure 12 is where a thin glass slide was located during deposition. The spectral transmittance of the gold covered slide was measured and plotted with a Beckman DK-1 spectrophotometer. Measurements were made over the major portion of the spectral band that most glasses are transparent to: 0.3μ to 3.5μ . The reflectance chart is shown in Figure 13.

Gold film thickness determinations were calculated from the change in weight of 0.5 mm. glass slides before and after deposition. An alternate method employed a Bausch and Lomb single beam interferometer attachment on a Lietz microscope; this method had an accuracy of approximately $\pm 0.05\mu$ whereas the weighing technique was accurate to within $\pm 0.01\mu$. Thickness as a function of resistance was plotted and used to monitor the rate of deposition of subsequent runs.



WAVELENGTH, μ

Figure 13 - Spectral Transmittance of a 0.2- μ Gold Film Coated on One Surface of a Thin Sheet of Glass

The tin oxide films were deposited on the aluminosilicate disks by indirect heating; i.e., a tungsten flat spiral filament was heated directly over stannous oxide (SnO) powder contained in a flat molybdenum pan. A measured amount of powder was evaporated by sublimation onto the disk which was 10 cm. above the source; the weight of the powder was calculated to provide the 0.2 μ film on the disk. The deposition procedure is terminated by exposing the SnO film to oxygen while the film is hot (800 F). Thus, the SnO film is oxidized and becomes predominantly SnO₂ as indicated by the color of the films; SnO films are brownish color while SnO₂ films are visibly transparent. The SnO₂ film thickness was confirmed by the single band interferometer-microscope to be approximately 0.2 μ .

C. Calibration of Apparatus

To simulate MRI experimental tests using the modified computer program, it was necessary to know the quantity of heat being transferred to the specimens. Likewise to correlate the experimental and analytical results, it was necessary to know the window surface temperatures as a function of time. Accordingly the radiant heater and the temperature grids were calibrated; this work is summarized in the following sections.

Radiation heater: The local radiant heat flux that impinges the test specimen is proportional to the emissive power, σT_H^4 , of the heater (see Eq. (5)), thus a high degree of accuracy in measuring T_H is required.

The temperature of the back side of the heater was detected by two chromel-alumel thermocouples, one for automatic control and the other for monitoring and recording. Since these thermocouples were on the back side of the heating element and are in contact with the refractory support block, they did not accurately sense the surface that was "seen" by the window. However, the back side and front side temperatures were related to each other and this relationship was determined experimentally by simultaneously monitoring the thermocouple and measuring the front side temperature, T_H , with an Ircon model 300 optical pyrometer. The resulting heater temperature calibration curve is shown in Figure 14.

Calorimeter: The function of the calorimeter was to measure the heat flowing through the window into the "cabin" and to aid in the calibration of the radiative and convective heaters.

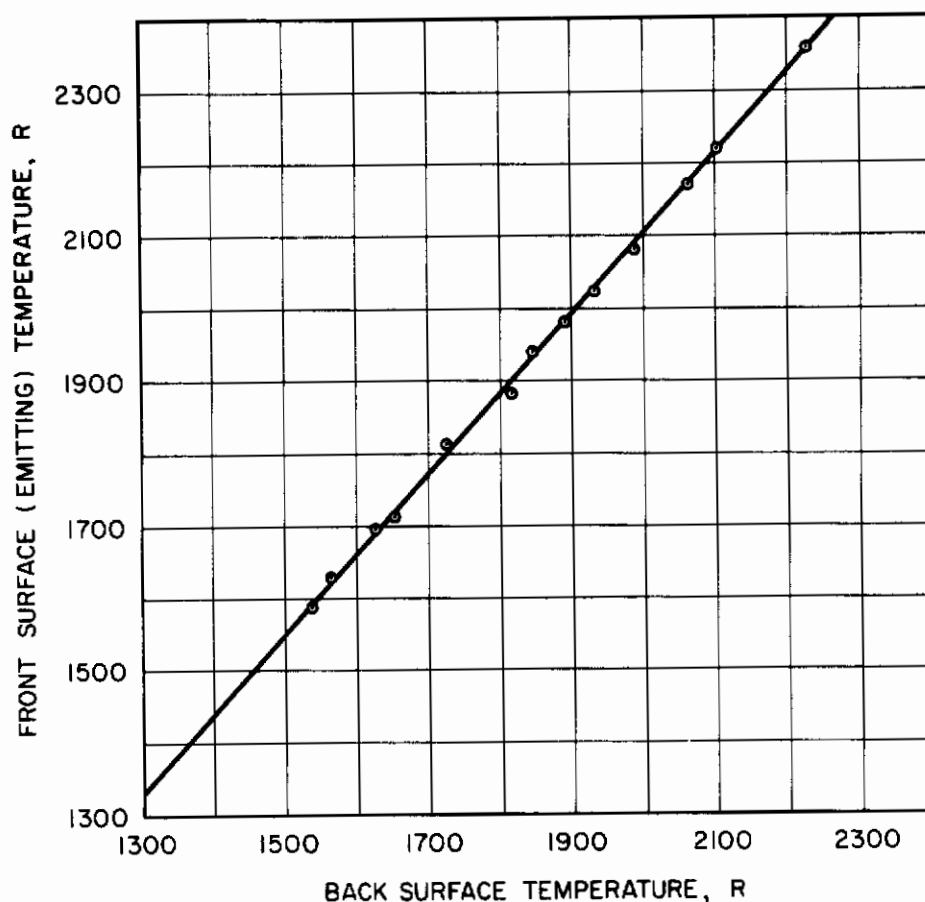


Figure 14 - Calibration of Radiant Heater Thermocouple Using an Optical Pyrometer

The heat flowing into the calorimeter is theoretically found by

$$q_{\text{net}} = \frac{\dot{w}(T_{\text{out}} - T_{\text{in}})C}{A} \quad (7)$$

where \dot{w} is the flow rate of the water, T_{in} and T_{out} are the inlet and outlet temperatures of the water, C is the heat capacity of the water, and A is the surface area of the calorimeter and is normal to the impinging heat flux.

The flow rate was determined by measuring the volume of water emptying into a graduated beaker in a timed interval. The water was supplied from a tank which was maintained at a uniform pressure to assure a uniform flow rate. The water temperature difference, $T_{\text{out}} - T_{\text{in}}$, was detected by a five junction chromel-constantan thermopile. At the operating temperature of the

calorimeter, approximately 80 F, the sensitivity of the thermopile was 0.1645 mv/ F. Substituting this value and other appropriate constants into Eq. (7) yields

$$q_{\text{net}} = 115.6 \dot{w} v \quad (8)$$

where the units are: q - Btu/hr·ft², \dot{w} - ml/min, and v - millivolts.

The proper selection of \dot{w} is important; the flow rate must be large enough that it can be accurately measured, but not so large that the thermopile signal is too weak to accurately sense. Figure 15 shows the experimental relationship between q_{net} , as determined by Eq. (8), and \dot{w} for a constant rate of heat into the calorimeter. The dependency of q_{net} on \dot{w} as $\dot{w} \rightarrow 0$ is probably due to the thermal junctions not being fully immersed at low flow rates. Similar data were recorded for other rates of heat input. Based on an analysis of these data, a flow rate of $\dot{w} = 320$ ml/min was selected and was attained by pressurizing the supply reservoir to 15 psig.

The calorimeter was calibrated by comparing the calculated quantity of heat absorbed by the water with the amount flowing to the calorimeter from a heated disk. The latter values were found at steady-state conditions by computing the heat transferred:

1. By conduction through a 0.134 in. Pyroceram* 9606 disk;
2. Across the gap from the Pyroceram disk to the calorimeter; and
3. Across the gap from a 1/32 in. type 304 stainless steel disk to the calorimeter.

The heat through the Pyroceram disk was computed as follows:

$$q = K \frac{T_1 - T_{11}}{\Delta x} \quad (9)$$

where K is the thermal conductivity of the disk and Δx is its thickness. The temperatures, T_1 and T_{11} , were measured with gold resistance grids deposited on the front and back surfaces, respectively.

* Trademark of Corning Glass Works, Corning, New York.

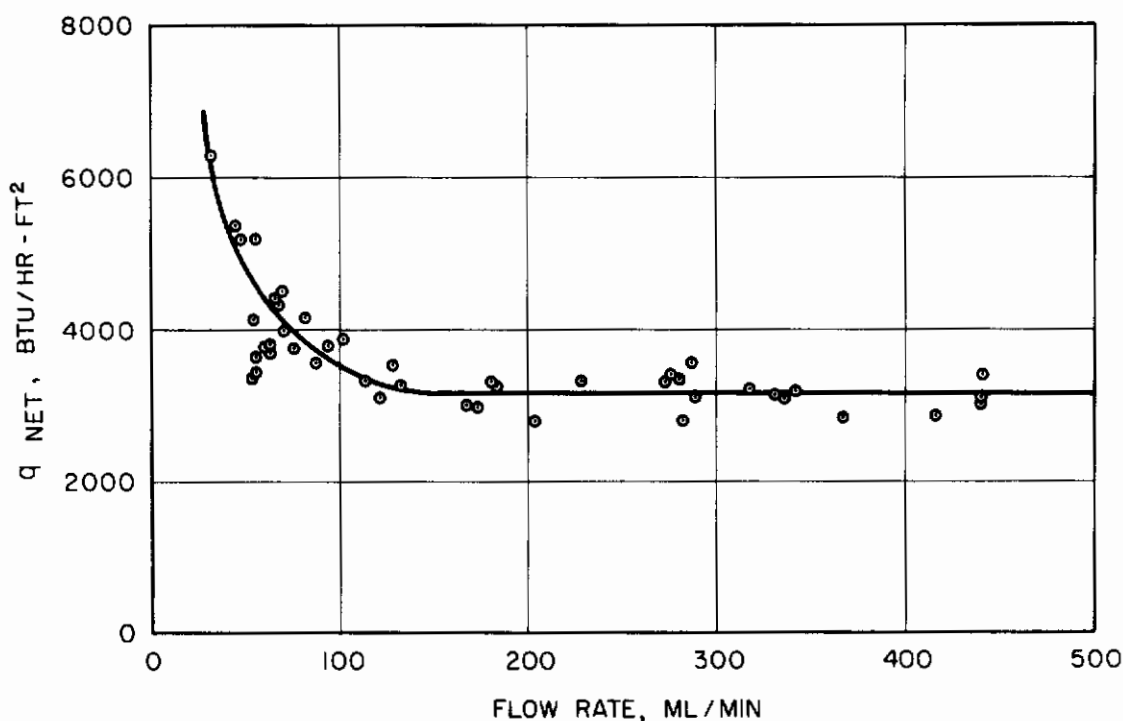


Figure 15 - Calorimeter Flow Rate Data for a
Constant Heat Flux

The heat convected and radiated from the back surface was determined by

$$q = h(T_{11} - T_C) + \sigma \epsilon (T_{11}^4 - T_C^4) \quad (10)$$

where h is the coefficient of heat transfer, ϵ is the emissivity of the disk, and T_C is the calorimeter temperature.

Published values of K and ϵ for Pyroceram 9606 were used to solve Eqs. (9) and (10). Values of ϵ of type 304 steel (oxidized at 1050 F and 1250 F) were experimentally determined.

Data for the three calibration runs are plotted in Figure 16. The curves indicate that Eq. (8) gives results that agree with experimental data and that an empirical coefficient to improve the correlation was not required.

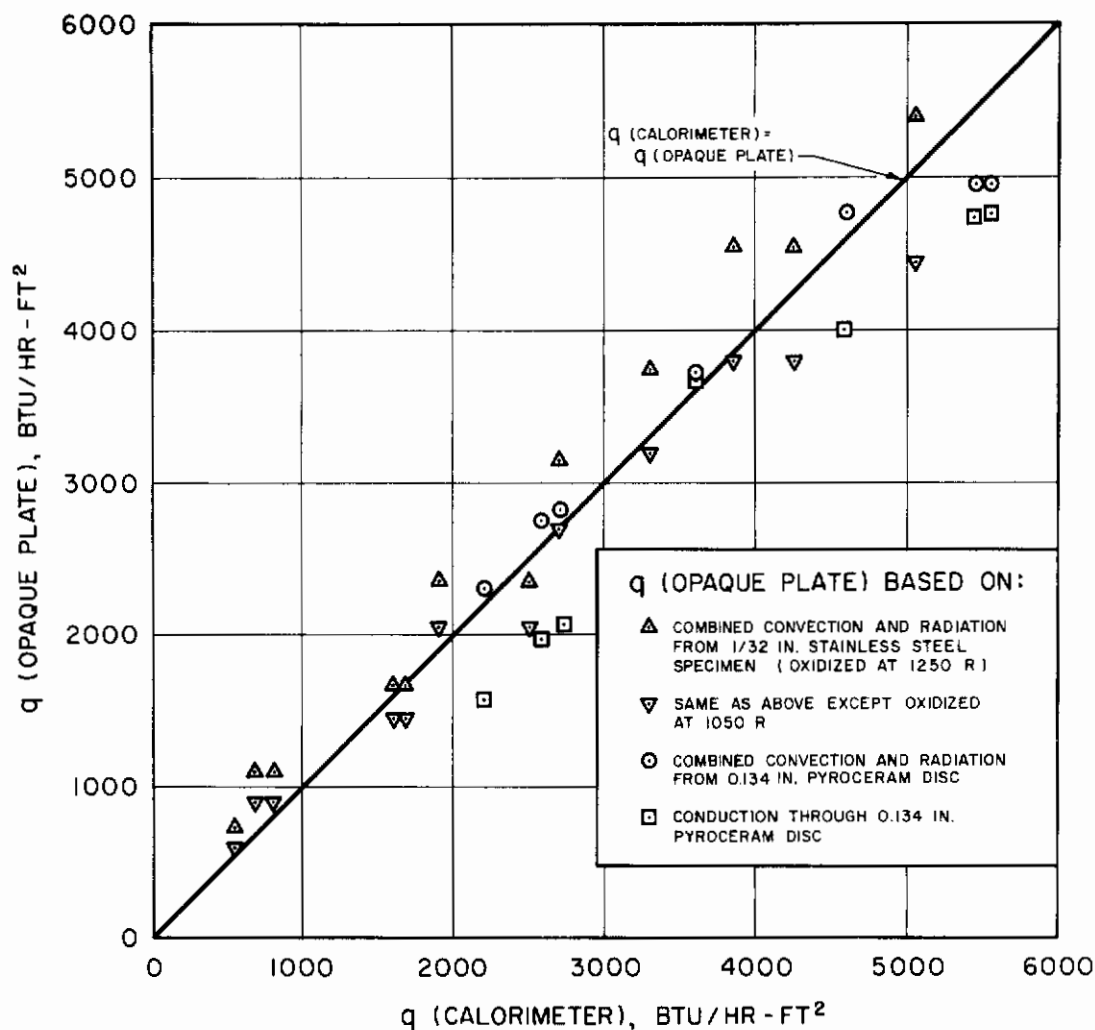


Figure 16 - Calorimeter Calibration

A further check of the calorimeter was made by using the apparatus to experimentally determine the thermal conductivity of type 304 stainless steel. Temperature gradients across a 0.236 in. thick disk were measured with surface thermocouples and steady-state heat fluxes were determined from calorimeter data. Average values of K are compared in Figure 17 with data by Deverall (Ref. 12), Przybycien (Ref. 13), and Ewing (Ref. 14).

Temperature sensors: Calibration of the temperature sensors on the window specimens was conducted in a Hoskins type FH2040 electric furnace. The window was mounted in a special fixture which secured and protected the specimen and provided ceramic insulators for the electrical leads. The fixture was constructed of stainless steel and was designed to damp out any temperature variations within the furnace. This was done by making the fixture sufficiently massive to have a high heat capacity and a slow thermal response to small fluctuations in the temperature of the furnace.

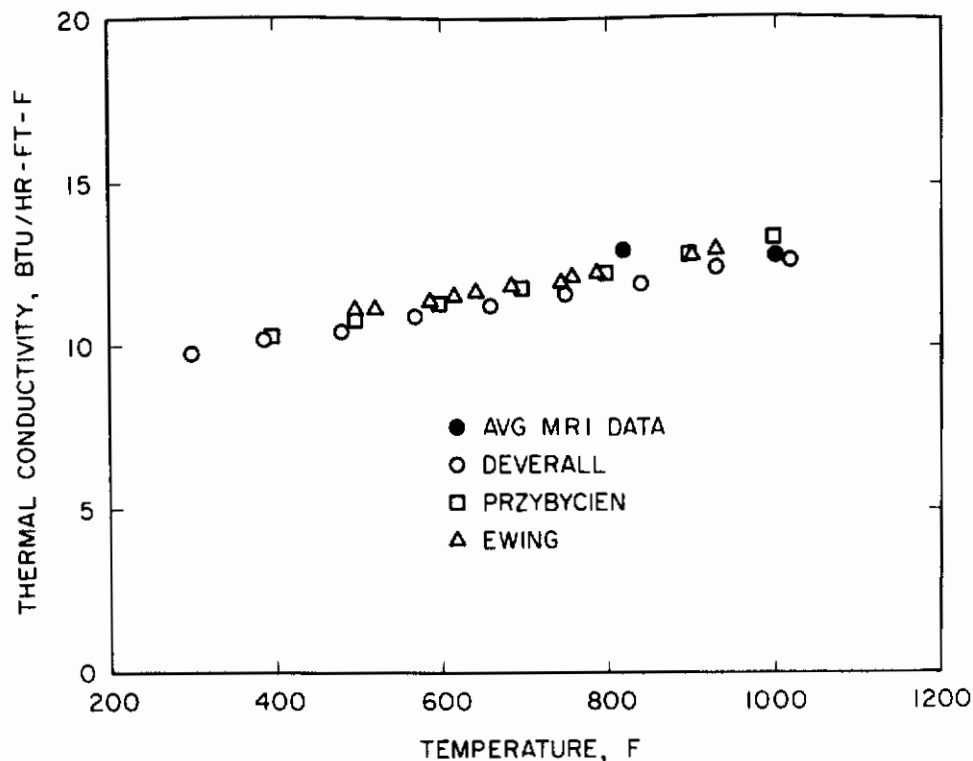


Figure 17 - Thermal Conductivity of Type 304 Stainless Steel as Determined by Transparent Boundary Apparatus

The specimen temperature was measured with a platinum - platinum-10 per cent rhodium thermocouple inserted into the fixture. The thermocouple reference junction was maintained at 32 F by means of an ice bath.

The power source for the sensor circuit was a Trygon Model HR 20-1.5 constant voltage DC power supply. The circuit was the same as that used in the experimental data runs. The sensors were connected in series. The current was determined by measuring the voltage drop across a precision 10 ohm resistance connected in series with the sensors. The sensor voltage junctions were connected to a multiple channel switch which, in turn, was connected to a Leeds and Northrup Model 8686 potentiometer. The output of the thermocouple was also connected to the switch.

After installation in the calibration fixture, the window specimen was placed in the furnace and heated to a temperature of 1000 F. This temperature was maintained for a period of 15 to 20 hr. to allow the gold temperature

sensors to stabilize. Calibration measurements were then made at stable temperatures incremented at approximately 200 F intervals from 1000 F to room temperature. Measurements were made of the voltage drop across each of the four temperature sensors, the voltage drop across the precision resistor, and the emf output of the thermocouple. At each temperature, as determined by the thermocouple, the resistance of each sensor was then computed from

$$R = \frac{V}{V_0} \times R_0 \quad (11)$$

where V is the voltage drop across the sensor, V_0 is the voltage drop across the precision resistor and $R_0 = 10$ ohms is the resistance of the precision resistor. The value of R versus temperature was then plotted for each sensor. A typical calibration curve is shown in Figure 18. Stability of the temperature sensors is indicated by the linearity of the calibration plots with straight lines characteristic of stable sensors. If, following calibration, the plot for any sensor was found to be nonlinear, the sensors were aged again and recalibrated. The calibration plots were used to determine the window temperatures during the data runs.

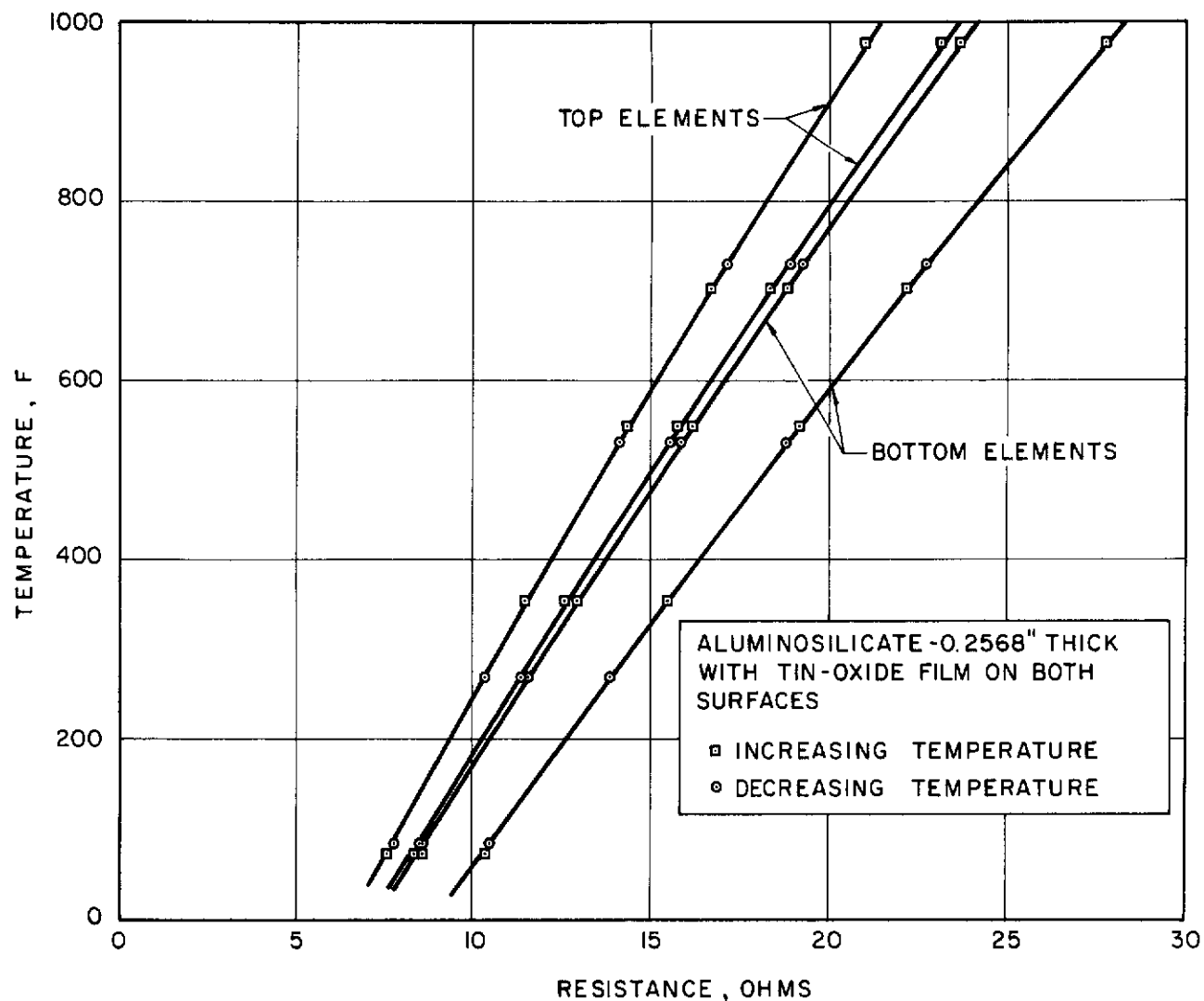


Figure 18 - Typical Calibration Curves for Window Surface Temperature Sensors

III. ANALYTICAL PROGRAM

A FORTRAN II computer program based on Gardon's theory was written by MRD for an IBM 7094 computer. Midwest Research Institute made modifications to a copy of the MRD program to enable it to simulate the experimental tests. Other changes were made to evaluate the program's accuracy, to facilitate data preparation, and to make the program compatible with FORTRAN IV monitoring systems. The modified program was written by MRI for the primary purpose of evaluating the MRD program; therefore, no attempt to document the modified version for general use has been made.

Gardon's theory, the MRD program, and the modified program are summarized below.

A. Theory of Heat Transfer Through Diathermanous Materials

Radiation calculations applicable to either opaque or perfectly transparent materials are relatively simple and are time proven. Such is not the case for diathermanous materials. Unlike opaque bodies, absorption by diathermanous materials takes place not just at the surface but in depth; unlike perfectly transparent materials, semitransparent materials partially absorb impinging radiation. The amount of absorption is dependent not only on the properties of the material but is also a function of its thickness.

Only in the last decade or so has the mechanism of radiant heat transfer in diathermanous materials been carefully analyzed. Before this time, radiation was either neglected or it was included by introducing an "equivalent" radiative thermal conductivity. For most applications, these fundamental approaches were satisfactory since net internal radiation is negligible at low temperatures and glass is essentially opaque to impinging radiation except when the source temperature is very high. However, for some conditions, such as those associated with molten glass during manufacture, the preliminary approach does not result in acceptable correlations between analytical and experimental data. Consequently, investigators have developed more sophisticated methods of analyzing the mechanism of radiative heat transfer in diathermanous materials at elevated temperatures.

The method accredited to Gardon includes considerable detail, yet the theory is sufficiently general that it is applicable to glass products and assemblies as well as to the manufacture of glass. For this reason, Gardon's theory has been employed in the subject computer program to aid in the study and design of hypersonic aircraft and spacecraft windows. His theory and related derivations which are presented in full in the literature (Ref. 15) are briefly discussed below.

The following general assumptions were made by Gardon:

1. The diathermanous material is a flat plate and is large enough for the net heat to be regarded as one-dimensional;*
2. The material is homogeneous and isotropic;
3. Reflection at the surface of the plate is governed by Fresnel's equations for dielectric materials; and attenuation of a monochromatic beam of radiation follows the Bouguer-Lambert law (see Eq. (A-1) in Appendix A).

The governing heat balance equations for a diathermanous material are similar to those for an opaque material, except that emission and absorption within the semitransparent medium must also be taken into account. The rate of internal emission of radiation per unit volume is dependent on the spectral volume emissive power, index of refraction, and absorption coefficient. Absorbed radiation includes that which originates from either an external source or from the material itself. External radiation is attenuated as it is transmitted through a diathermanous plate and is partially reflected back through the plate when it strikes the opposite internal surface. The reflected beam travels back and forth continuously giving up energy until its intensity diminishes to zero. The rate of reabsorption (of internally emitted radiation) at a given element is dependent on the rate of emission at all other elements. Like the absorption of external radiation, reabsorption takes place as the beams are transmitted back and forth through the material.

The heat transfer equations developed by Gardon were the basis for those employed in the MRD computer program. The primary difference between the two is that Gardon's equations are for symmetrical heating and cooling and those used by MRD for unsymmetrical heating and cooling. The MRD equations are summarized in the following section; detailed explanations and derivations are given in the report by Lis which describes the program (Ref. 16).

B. MRD Computer Program

The function of the MRD computer program is to evaluate the governing equations which are:

* Gardon justifies this assumption as follows: "Energy transfer by diffuse radiation is a three-dimensional process. However, with temperature gradients existing in one dimension only, the net energy transfer is one-dimensional."

$$\left. \begin{aligned} \frac{\Delta T_i}{\Delta t} = \frac{1}{\rho C} \sum q_i'''(T_j) + \frac{K}{\rho C} \cdot \frac{\Delta \left(\frac{\Delta T}{\Delta x} \right)}{\Delta x} = \frac{1}{\rho C} \left[Q_A(x_i) - Q_E(x_i) + Q_R(x_i) \right] \\ + \frac{K}{\rho C} \cdot \frac{\Delta \left(\frac{\Delta T}{\Delta x} \right)}{\Delta x} \end{aligned} \right\} \quad (12)$$

$$\frac{\Delta T_1}{\Delta t} = \frac{1}{\rho C} \left\{ \sum q_1'''(T_j) + \frac{1}{\frac{\Delta x}{2}} \left[(q_1'') + (1 - \rho_{Hm}) W_{Hm} - \epsilon_m W_{Bm}(T_1) - K \frac{\Delta T_1}{\Delta x} \right] \right\} \quad (13)$$

$$\frac{\Delta T_{11}}{\Delta t} = \frac{1}{\rho C} \left\{ \sum q_{11}'''(T_j) + \frac{1}{\frac{\Delta x}{2}} \left[-h_c(T_{11} - T_C) - \epsilon_m W_{Bm}(T_{11}) + K \frac{\Delta T_{11}}{\Delta x} \right] \right\} \quad (14)$$

where i represents an internal element, 1 represents the front surface and 11 represents the back or cabin surface as shown in Fig. 19. The radiation fluxes and functions used in the above equations are defined in the following paragraphs.

Radiation fluxes: The flux absorbed at x_i from external radiations is

$$Q_A(x_i) = 2 S n^2 \sum_m^m \gamma_{\lambda_m} W_{H\lambda_m} \phi \quad (15)$$

where $S = 1$ for internal elements and $S = 1/2$ for surface elements. The flux radiated from x_i is

$$Q_E(x_i) = 4n^2 \sum_m^m \gamma_{\lambda_m} W_{B\lambda_m}(x_i) \quad (16)$$

The energy reabsorbed at x_i from the other elements is

$$Q_R(x_i) = 2 S n^2 \sum_m^m \gamma_{\lambda_m}(x_i) \left[\sum_{L=1}^L \gamma_{\lambda_m}(y) W_{B\lambda_m}(y) \hat{P} \Delta y \right] \quad (17)$$

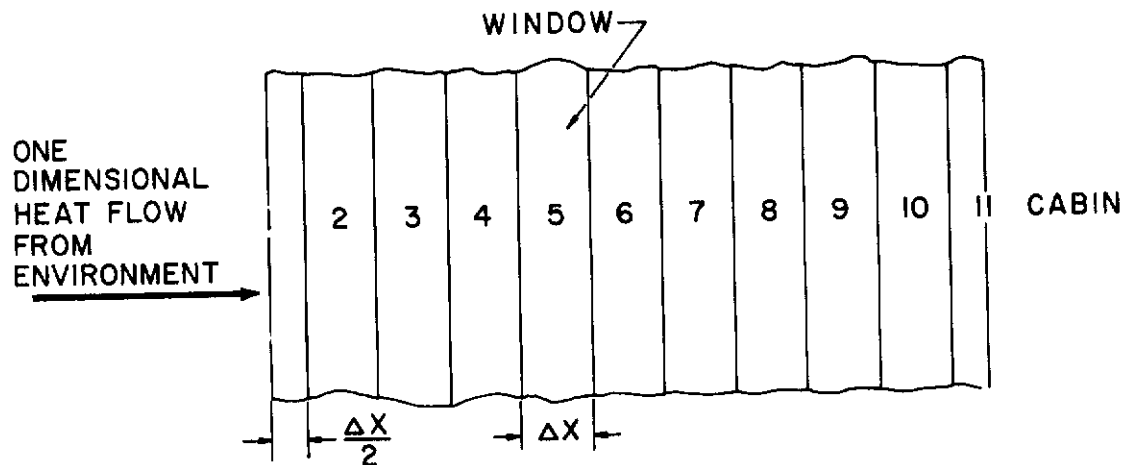


Figure 19 - Window Cross Section

The absorbed external radiant flux in wavelengths that the glass is opaque to is

$$(1 - \rho_{Hm}) W_{Hm} = (1 - \rho_{Hm}) \left[1 - p_m(T_H) \right] \left[\epsilon_g \sigma T_H^4 \right] \quad (18)$$

The heat that is radiated from the glass in "opaque" wavelengths is

$$\epsilon_m \left[W_{Bm}(T_1) \right] = \epsilon_m \left[1 - p_m(T_1) \right] \left[\sigma T_1^4 \right] \quad (19)$$

The amount of external radiation that impinges the glass at wavelengths that glass is transparent to is

$$W_{H\lambda_m} = p_{\lambda_m} \epsilon_g \sigma T_H^4 \quad ; \quad (20)$$

the "transparent" energy that is radiated from element x is

$$W_{B\lambda_m}(x) = p_{\lambda_m} \sigma T_x^4 \quad (21)$$

Auxiliary functions: The functions $\phi(x)$ and $\hat{P}(x,y)$ used in the above equations are given by

$$\phi = \sum_{\alpha=0}^{\alpha_{cr}} \tau' \left\{ e^{-\gamma_{\lambda} x \sec \alpha} + \frac{e^{-2\gamma_{\lambda} L \sec \alpha}}{1 + \frac{\tau'_{||}}{\tau'_{\perp}}} \left[\frac{\rho'_{\perp} (\rho'_{\perp} e^{-\gamma_{\lambda} x \sec \alpha} + e^{\gamma_{\lambda} x \sec \alpha})}{1 - (\rho'_{\perp})^2 e^{-2\gamma_{\lambda} L \sec \alpha}} + \right. \right. \\ \left. \left. \frac{\tau'_{||}}{\tau'_{\perp}} \cdot \frac{\rho'_{||}}{1 - (\rho'_{||})^2 e^{-2\gamma_{\lambda} L \sec \alpha}} \cdot \left(\rho'_{||} e^{-\gamma_{\lambda} x \sec \alpha} + e^{\gamma_{\lambda} x \sec \alpha} \right) \right] \sin \alpha \Delta \alpha \right\} \quad (22)$$

and

$$\hat{P} = P + \sum_{\alpha=0}^{\pi/2} \tan \alpha \cdot e^{-\gamma_{\lambda} |x-y| \sec \alpha} \Delta \alpha \quad (23)$$

where

$$P = \sum_{\alpha=0}^{\pi/2} \left\{ \left[P'_1 e^{-\gamma_{\lambda} (L-x) \sec \alpha} + P'_2 e^{-\gamma_{\lambda} (L+x) \sec \alpha} \right] e^{-\gamma_{\lambda} (L-y) \sec \alpha} \right. \\ \left. + \left[P'_1 e^{-\gamma_{\lambda} x \sec \alpha} + P'_2 e^{-\gamma_{\lambda} (2L-x) \sec \alpha} \right] e^{-\gamma_{\lambda} y \sec \alpha} \right\} \tan \alpha \Delta \alpha. \quad (24)$$

Miscellaneous functions: Other functions used in the above equations are

$$\tau' = 1/2 (\tau'_{\perp} + \tau'_{||}) \quad (25)$$

$$\tau'_{\perp} = 1 - \rho'_{\perp} \quad (26)$$

$$\tau'_{||} = 1 - \rho'_{||} \quad (27)$$

$$\alpha_{cr} = \sin^{-1}\left(\frac{1}{n}\right) \quad (28)$$

$$\rho'_{\perp} = \frac{n \cos \alpha - (1-n^2 \sin^2 \alpha)^{1/2}}{n \cos \alpha + (1-n^2 \sin^2 \alpha)^{1/2}} \quad (29)$$

$$\rho'_{||} = \frac{(1/n) \cos \alpha - (1-n^2 \sin^2 \alpha)^{1/2}}{(1/n) \cos \alpha + (1-n^2 \sin^2 \alpha)^{1/2}} \quad (30)$$

$$P'_1 = 1/2 \left[\frac{\rho'_{\perp}}{1-(\rho'_{\perp})^2 e^{-2\gamma_{\lambda} L \sec \alpha}} + \frac{\rho'_{||}}{1-(\rho'_{||})^2 e^{-2\gamma_{\lambda} L \sec \alpha}} \right] \quad (31)$$

$$P'_2 = 1/2 \left[\frac{(\rho'_{\perp})^2}{1-(\rho'_{\perp})^2 e^{-2\gamma_{\lambda} L \sec \alpha}} + \frac{(\rho'_{||})^2}{1-(\rho'_{||})^2 e^{-2\gamma_{\lambda} L \sec \alpha}} \right] \quad (32)$$

C. Modified Computer Program

Numerous modifications to a copy of the MRD program were made to provide correlation with the experimental program, to evaluate the program's accuracy and running time, and to facilitate data preparation for the test cases.

Modifications to give correlation with the experimental test conditions: Changes were made to the program to enable it to duplicate evaluation tests performed with the experimental apparatus. These included:

1. An option to accept constant radiation and/or convection heat input data;

2. The introduction of configuration factors to compensate for the finite-sized experimental radiant heater;

3. A revision of the upper limit of α from 90 degrees to an angle less than 90 degrees which corresponds to the geometry of the radiant heater; and

4. Changes in the heat flux equations at the two boundaries to account for differences between the experimental and the analytical heat sinks (i.e., the water cooled back plate vs. the cabin of the hypothetical vehicle) and similar differences.

Modifications to improve program accuracy and to reduce computational time: A preliminary review of the theory and computational techniques employed in the program indicated that certain changes could significantly improve the program while others might have only a negligible effect. Therefore, all promising modifications were incorporated into the modified program for analysis to determine their relative merits.

The most significant improvement was to allow the radiation interchange terms, Q_A , Q_E , and Q_R given by Eqs. (15), (16) and (17) to be integrated over more than two wavelength bands. This modification makes it possible to approximate absorption coefficient curves with a step function to a reasonable degree of accuracy.

The effect of integrating over more than two wavelength bands was evaluated on the computer; the results of one study, in which a 96 per cent silica window was theoretically irradiated with intense short wavelength energy, are plotted in Figure 20. The five-band approximation yields an equilibrium temperature that is 265 F more accurate than the two-band approximation. The curve also indicates that little additional improvement would be attained by integrating over six or more increments. Although this was a representative test case, the actual improvement resulting from this modification will vary from case to case depending on the type of window material, its thickness, the heater temperature, etc.

A related program modification accounts for the fact that diathermanous materials are opaque below a certain wavelength, usually approximately 0.5μ . When the sun is the source of radiation, this opacity should not be ignored since 24 per cent of solar energy is emitted at wavelengths less than 0.5μ ; therefore, the modified program includes an opaque region on both sides of the transparent band.

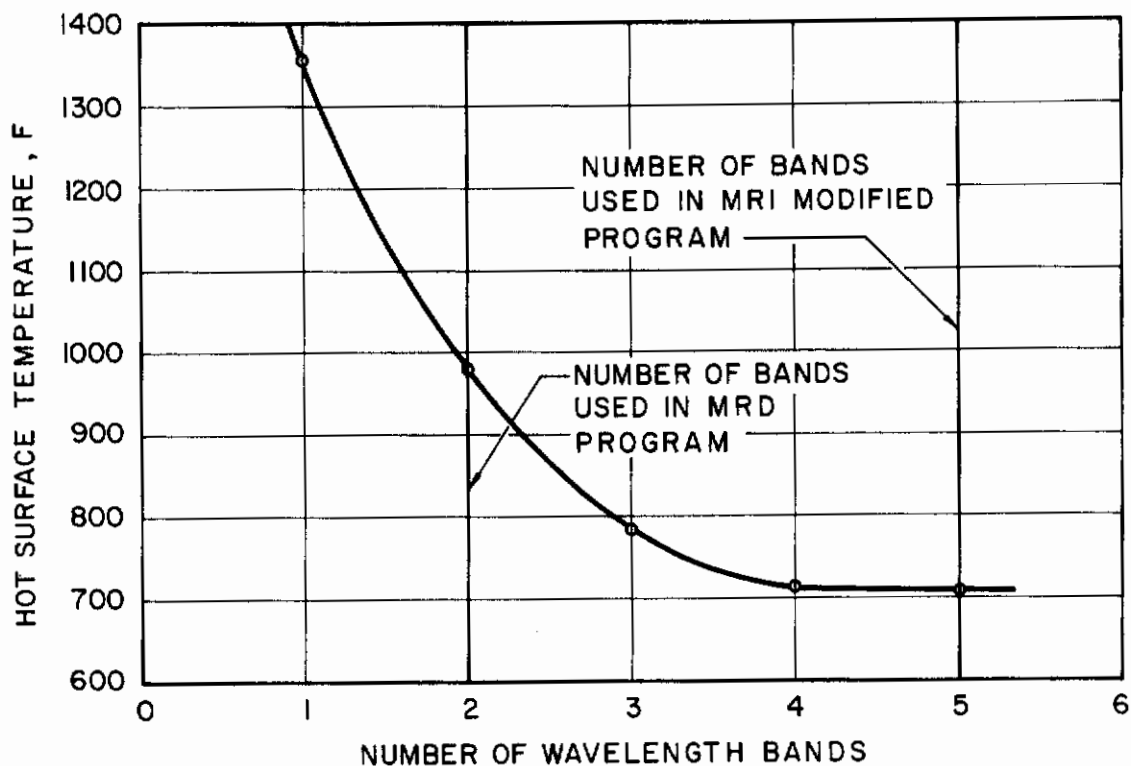


Figure 20 - Influence of Number of Wavelength Bands on Program Accuracy

The final major refinement which can result in a significant increase in accuracy was to allow the following glass properties used by the program to be a function of temperature: ρC , K , n , and " $1-\rho$ ". For temperatures below 1200 F, γ is practically unrelated to temperature; however, the temperature-dependent capability was retained for high temperature studies.

Although it was deemed that evaluation of the program's accuracy was the primary objective of this study, the following methods of reducing computational time were among those investigated and/or carried out:

1. Conversion of the program to FORTRAN IV to take advantage of input/output buffering and to facilitate altering array sizes;
2. Determination of running time as a function of size of various tables;
3. Suppression of unnecessary "transparent" calculations when the opaque option is used;
4. Elimination of redundancy in computing ϕ and \hat{P} values;

5. Comparison of explicit and implicit integration of difference equations;

6. Modification of the simultaneous equation solutions to search each row or column for the maximum pivotal element before reducing the matrix; and

7. Determination of accuracy and running time when internal reflectances are simplified by dropping the use of directional values.

The above investigations resulted in some minor improvements in the program.

Modifications to facilitate data preparation: The data requirements of the program being evaluated were unnecessarily complicated; therefore, considerable effort was devoted to simplifying the input routine. The invariable relationship between per cent of blackbody energy and the product of temperature and wavelength was changed from an input table to an integral part of the main program. Likewise, thermal and optical properties of glasses commonly used in aircraft window assemblies were stored in the program making it unnecessary for the user to repetitiously compile and prepare data each time the program is run. Data for soda lime, borosilicate, aluminosilicate, 96 per cent silica, and fused silica were compiled, calculated and used in the MRI evaluation runs.

These and similar MRI modifications, if permanently incorporated into the program, would permit the program to be used by personnel who are not thoroughly acquainted with the theory and numerical techniques employed by the program; and would significantly reduce the time required to prepare input data, minimize data errors, and reduce the possibility of using incorrect or obsolete glass properties.

D. Comparison of the MRD and Modified Computer Programs

The primary purpose of modifying the MRD program was to make it possible to simulate experimental conditions on the computer. Care was taken to insure that the modifications did not alter any of the basic program theory or numerical techniques. As a check, identical problems were run with each program and the results compared. The time-temperature relationships were in close agreement; however, deviations in q''' at certain nodes were noted. It was determined that these differences were caused by random numbers that were introduced by a faulty logic test in the MRD program. Since the programs were using different systems (FORTRAN IV and FORTRAN II), it was impossible to obtain agreement until the program error and resulting random numbers were eliminated. A discussion of the faulty logic test in the MRD program follows.

One of the terms in the expression for q''' is of the following form:

$$\int_0^L \gamma_\lambda W_{B\lambda}(y) dy \int_0^{\frac{\pi}{2}} e^{-\gamma_\lambda |x-y| \sec \alpha} \left(\frac{1 - e^{-\gamma_\lambda \delta \sec \alpha}}{\delta x} \right) \sin \alpha d\alpha \quad (33)$$

When this integral is evaluated numerically, it is necessary to set the exponential $e^{-\gamma_\lambda |x-y| \sec \alpha}$ to zero when y equals x . The MRD program contains a sequence of statements which test for equality of x and y and evaluates the exponential accordingly. However, unless x and y are exactly equal, the exponential term is not suppressed.

It can happen as a result of roundoff that values of x and y which should be equal will not be exactly equal, since x is summed in increments of Δx and y is summed in increments of $2\Delta x$. This is illustrated with an example where four significant digits are carried and Δx is 0.03333.

<u>Node No.</u>	<u>x</u>	<u>y</u>
1	0.	0.
2	0.03333	
3	0.06666	0.06666
4	0.09999	
5	0.13332 → 0.1333	0.13332 → 0.1333
6	0.16663 → 0.1666	
7	0.19993 → 0.1999	0.19996 → 0.2000
8	0.23323 → 0.2332	
9	0.26653 → 0.2665	0.26666 → 0.2667
10	0.29983 → 0.2998	
11	0.33313 → 0.3331	0.33336 → 0.3334

Thus, for nodes 7, 9 and 11, y can never be exactly equal to x because of roundoff. Hence, the computer would evaluate the term $e^{-\gamma_\lambda |x-y| \sec \alpha}$ with $|x-y|$ being a very small number and the exponential will be close to unity instead of zero.

Instead of testing whether y equals x , it is better to test whether the absolute value of the difference $|x-y|$ is less than $\frac{\Delta x}{2}$. If so, then x and y represent the same node and the exponential term can be set to zero.

This logic correction was made and the corresponding output deviations between the modified program and the MRD program were essentially eliminated as a result. Furthermore, this correction also improved the q''' distribution through the window. This is seen in Figure 21 where "before" and "after" computer output data are presented. Before making the logic correction, q''' at nodes 9 and 11 differed considerably from values at nodes 8 and 10. These discontinuities, which theoretically should not exist, are seen to have diminished considerably after the program change was made. The remaining fluctuations are caused in part by evaluating \hat{P} in Eq. (23) at every other y/x instead of at every y/x .

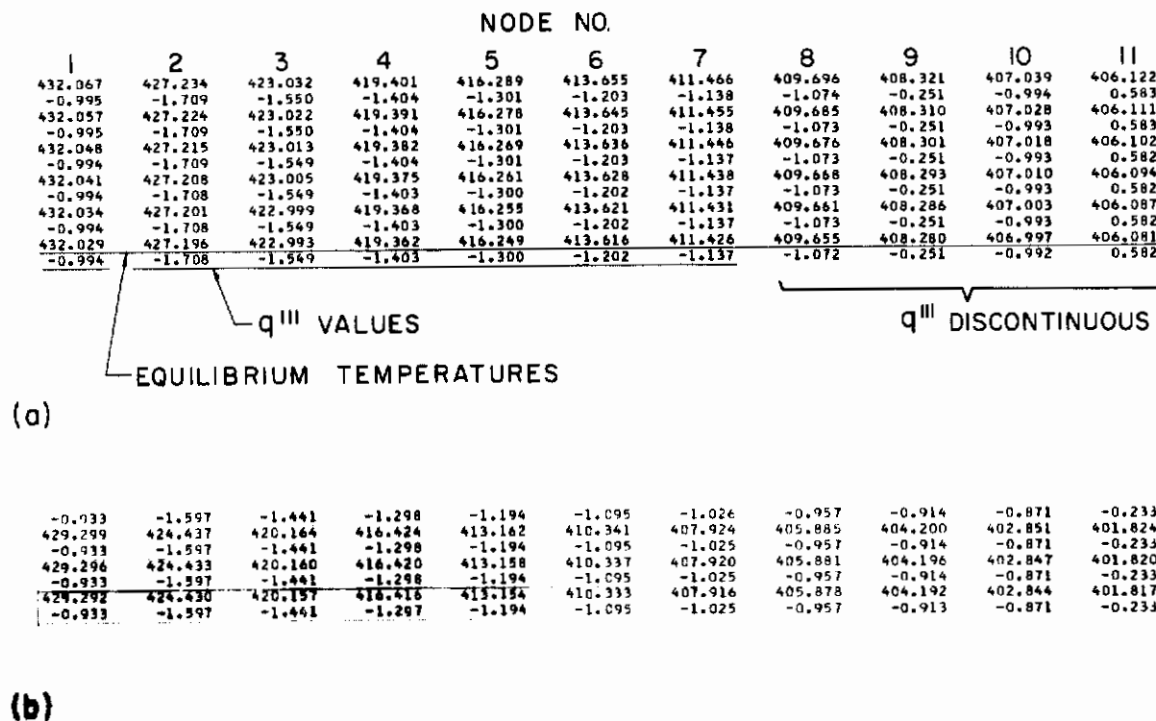


Figure 21 - Outout Data Before (a) and After (b) Correcting Faulty Test

IV. EVALUATION OF COMPUTER PROGRAM

Over 100 test conditions were analyzed both in the laboratory and on the computer to aid in the evaluation of the computer program. The parameters included thickness, type of window material, heat flux, surface temperature, type of film material, and film location (e.g., front window surface). A description of the tests and analysis of the results are given in the following sections.

A. Experimental Tests

Diathermanous disks were heated by radiation, convection, and combined radiation and convection. The substrate materials tested were 96 per cent silica and aluminosilicate; the films were gold and tin oxide. The coated windows had films on either the front side or the back side, or on both surfaces. The disks were 1/8 in., 1/4 in., and 5/16 in. thick and the films were 0.2 μ thick.

The surface temperatures were monitored and recorded at thermal equilibrium and the net heat flux was calculated for each test. The results are plotted in Appendix C. A visual inspection of Figure C-1 indicates the window absorbed less heat from impinging radiation than from an equivalent amount of convection. Whereas all of the heat convected to the glass was absorbed at the surface, some of the radiant energy was transmitted through the window and into the "cabin" and some eventually escaped back into "space." Theoretically, the transparency of glass increases as the radiant source temperature increases and consequently a window is heated to a lower equilibrium temperature for a given intensity of thermal radiation. The energy data for the low temperature source (when $h = 9/16$ in.) and the energy data for the high temperature source (when $h = 8$ in.) shown on the graph subscribe to this logic.

B. Empirical Calculations

Before proceeding to evaluate the computer program, confidence in the experimental data was gained by comparing the results to those obtained empirically.

Empirical methods of analyzing heat transfer in glass are time proven and are still used to given satisfactory solutions to many practical problems involving transparent materials. These methods use effective emissivity and thermal conductivity values in conjunction with the elementary Fourier equation

for one-dimensional conduction. The effective values are determined from experimental measurements and/or theoretical considerations. The emissivity of transparent materials has been studied by numerous investigators. In one study, Gardon computed spectral hemispherical emissivity as a function of dimensionless thickness and total hemispherical emissivity (effective emissivity) as a function of thickness and temperature. The latter relationship is reproduced in Figure 22 (Ref. 4).

Empirical relationships between the surface temperature of a diathermanous disk and the impinging one-dimensional convective heat flux are given in the following equations. The net heat flow through a disk at equilibrium is

$$q_{\text{net}} = h(T_{11} - T_C) + \sigma T_{11}^4 \epsilon f(\epsilon) - \sigma T_C^4 \quad (34)$$

where h is the coefficient of heat transfer between the window and the calorimeter, ϵ is the emissivity of an infinitely thick disk at T_{11} , and $f(\epsilon)$ is a factor that accounts for the effect of thickness and temperature on the emissivity of a diathermanous material. Values of $\epsilon f(\epsilon)$ for soda lime as determined by Gardon are plotted in Figure 22. Convective heat flow into the disk is given by

$$q_1'' = q_{\text{net}} + \sigma T_1^4 \epsilon f(\epsilon) - \sigma T_R^4 \quad (35)$$

where σT_R^4 , in the case of no radiant heater, is the radiant flux from the environment at room temperature, T_R .

The use of the above empirical equations is illustrated in the following example:

material - 96 per cent silica

$X_{11} - X_1 = 5/16$ in. (specimen thickness)

$X_C - X_{11} = 0.175$ in. (air gap between specimen and calorimeter)

$T_{11} = 830$ F

$T_C = 70$ F

$T_R = 75$ F

Problem: Find the net heat flow and the impinging convective heat flow.

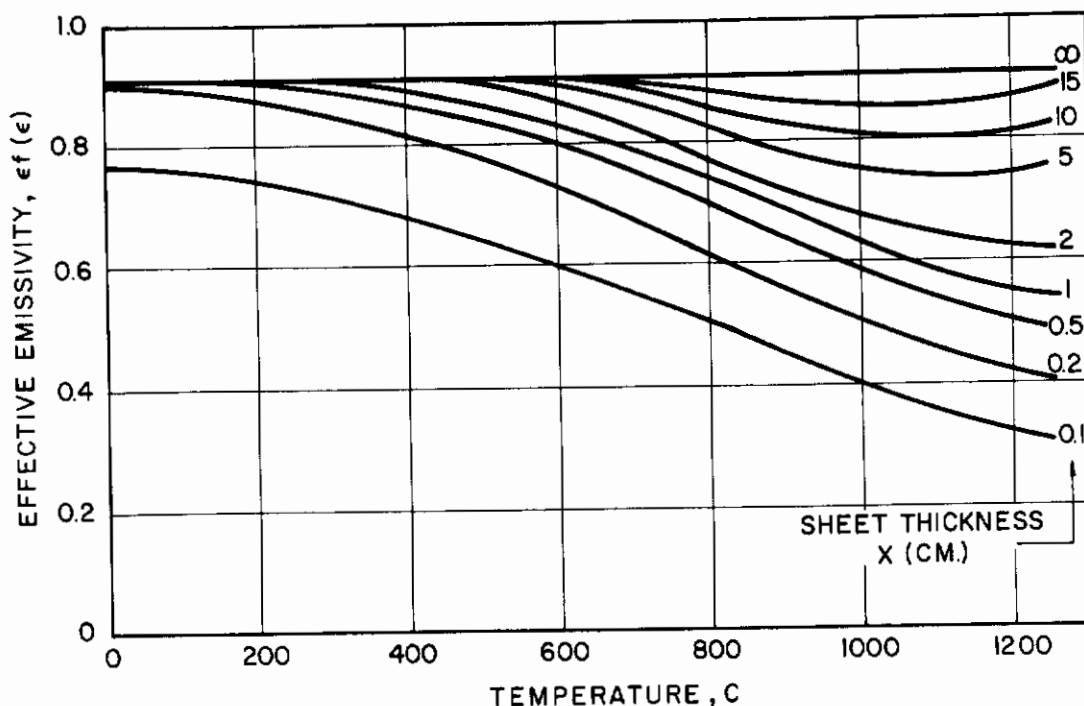


Figure 22 - Effective Emissivity of Soda Lime Glass as Determined by Gardon. (Ref. 4)

The 0.175 in. air gap is too narrow to permit an appreciable degree of natural convection; therefore, the coefficient of heat transfer is calculated as follows

$$h = \frac{K_{\text{air}}}{X_C - X_{11}} = \frac{0.0233}{0.175/12} = 1.60 \text{ Btu/hr} \cdot \text{ft}^2 \cdot \text{F}$$

where K_{air} is the thermal conductivity of air at the average temperature of T_C and T_{11} .

The emissivity at T_{11} is approximated by first dividing the abscissa of the $(1 - \rho_H)_\lambda$ curve for 96 per cent silica into a finite number of $\Delta\lambda$ increments and evaluating $(1 - \rho_H)_\lambda \Delta P_\lambda$ for each increment where ΔP_λ is the per cent of blackbody energy emitted at T_{11} between the wavelengths λ and $\lambda + \Delta\lambda$. The value of ϵ is then found as follows

$$\epsilon \approx \sum (1 - \rho_H)_\lambda \Delta P_\lambda. \quad (36)$$

For a surface temperature of 830 F, the emissivity of 96 per cent silica was found to be 0.86. The factor $f(\epsilon)$ was determined indirectly from Figure 22 assuming 96 per cent silica and soda lime curves to be similar. For a thickness of 5/16 in. and a temperature of 830 F, $f(\epsilon)$ was found to be 0.953.

Substituting the values of T_{11} , T_C , h , ϵ and $f(\epsilon)$ into Eq. (34) yields

$$q_{\text{net}} = 1230 + 3880 - 148 = 4962 \text{ Btu/hr}\cdot\text{ft}^2$$

The temperature gradient, $T_1 - T_{11}$, is calculated as follows

$$T_1 - T_{11} = \frac{q_{\text{net}} (X_{11} - X_1)}{K} = \frac{4962 \times 5/16}{0.0181 \times 57.8 \times 12} = 123 \text{ F}$$

where K is the effective thermal conductivity of 96 per cent silica based on experimental measurements (see Appendix A). As a check, ΔT was found from curves which were determined in the experimental program for the same test conditions. The experimental and analytical values of $T_1 - T_{11}$ agreed to within 5 F as shown in Figure 23. T_1 is found by adding ΔT and T_{11} and therefore is 953 F.

The effective emissivity is determined for x_1 at T_1 as previously described. Substituting q_{net} , T_1 , $\epsilon f(\epsilon)$ and T_R into Eq. (35) and solving yields $q_1'' = 10,504 \text{ Btu/hr}\cdot\text{ft}^2$.

The graph in Figure 24 compares the empirical solutions as described above with the experimental results which were discussed in the previous section. The excellent agreement tends to substantiate the validity of the experimental program.

C. Computer Program Results

The test conditions for the experimental production runs described in Section IV-A were simulated with the computer program. The results of one set of tests are shown in Figure 24 along with the experimental and empirical results which were previously discussed. The correlation between the analytical and experimental results is seen to be poor.

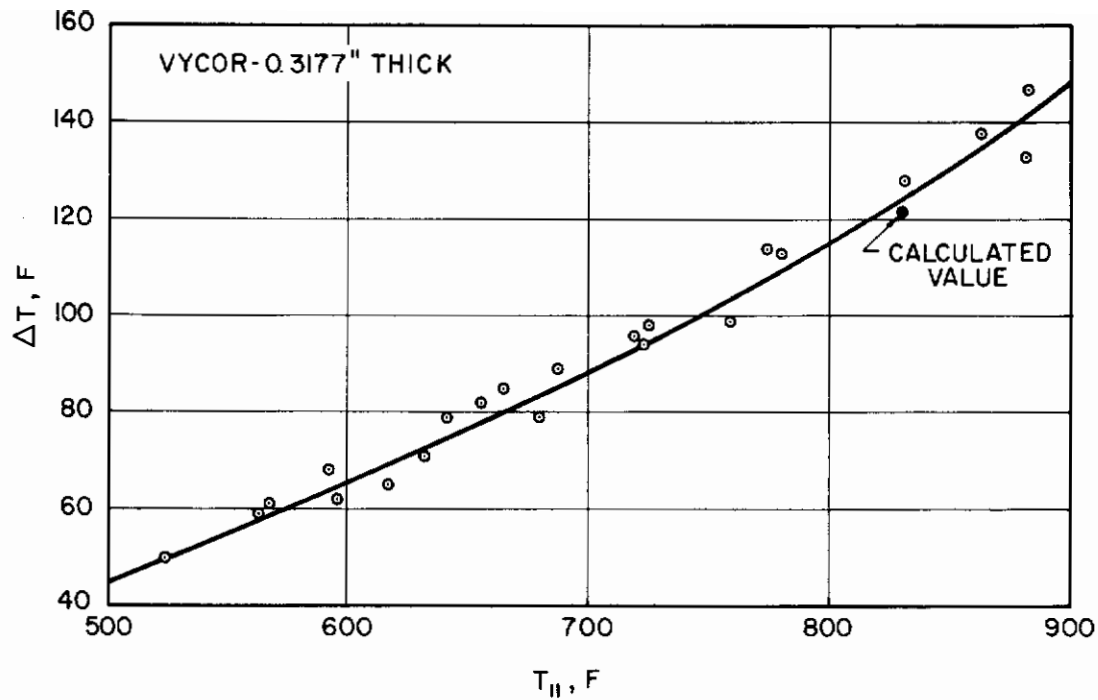


Figure 23 - Experimental Temperature Gradient Data

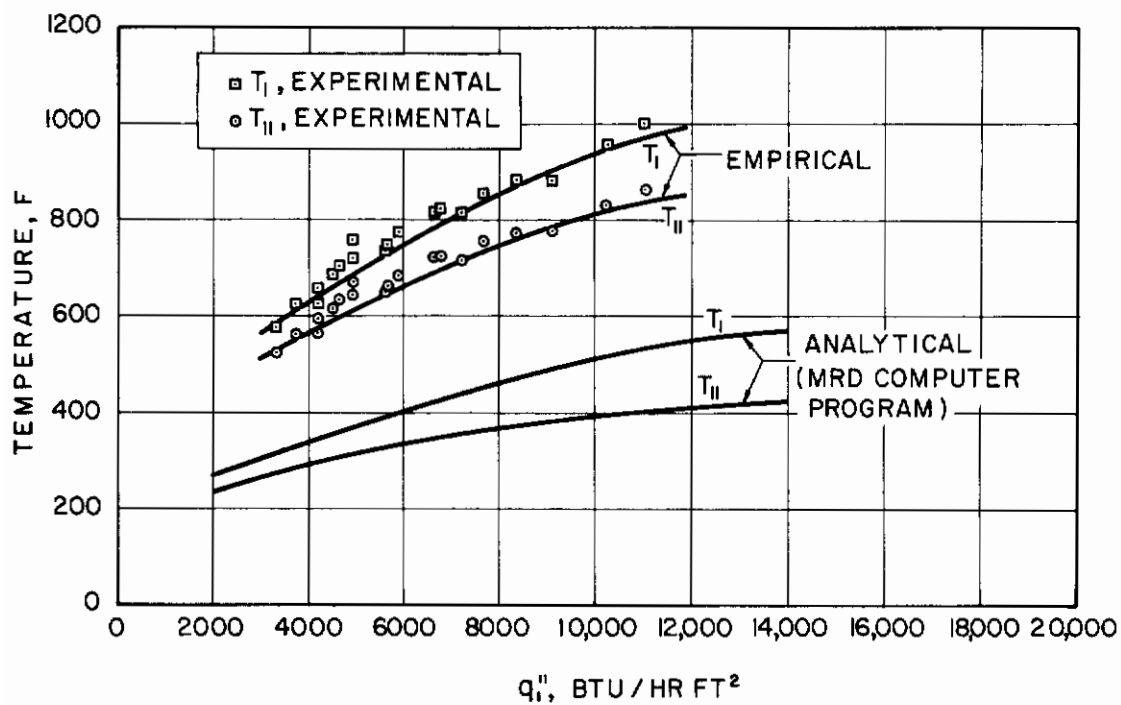


Figure 24 - Comparison of Analytical, Empirical and Experimental Data

Additional runs were made in an attempt to isolate the area(s) of disagreement. A stainless steel "window" was experimentally tested and numerically analyzed "by hand" and on the computer. The resulting equilibrium temperatures were essentially identical in each case; therefore, it was concluded that any existing significant errors must be associated with the transparent theory and not the opaque theory.

Since the analytically and experimentally determined temperature gradients for a given heat flux through the window are approximately equal (see Figure 24), it was concluded that the values used by MRI for true thermal conductivity of glass were reasonably accurate. This was confirmed in subsequent computer tests in which K was varied from one run to the next. The result was that the temperature gradients varied, but the average glass temperature was not appreciably affected and remained considerably different from the average window temperature of the corresponding experimental tests.

At the termination of all scheduled production runs it could only be concluded that the computer results did not agree with the empirical or experimental results. Tests specially designed to evaluate the computer program are discussed in the following section.

D. Program Evaluation

A test of the transparent theory employed in the MRD program was made by analyzing a transparent material using the opaque program option and then analyzing a hypothetical glass having negligible transparency ($\gamma \gg 1$) using the transparent program option. The test conditions and the glass properties were identical, except for the γ values, and were selected such that the resulting equilibrium temperatures should be identical. Run No. 112 used the opaque option and run No. 113 simulated an opaque window but used the unproven transparent option; the convective input was 4000 Btu/hr.ft² in each case.

The results did not correlate -- the temperatures of the two surfaces for Run No. 112 were 515 F and 552 F; the values for Run No. 113 were 276 F and 320 F. Since the validity of the opaque option has previously been established, it can be concluded that for this set of conditions the general MRD program (transparent option) yields results that contain significant errors.

Next, an evaluation test using a conventional window material, 96 per cent silica, was made. A 5/16 in. specimen was heated by convection; the heat flux rate was 12,000 Btu/hr.ft². The equilibrium temperatures and radiation interchange terms computed by the MRD program are as follows:

<u>Node No.</u>	<u>Temp. (K)</u>	<u>q''' (watts/cm²)</u>
1	557	-3.727
2	541	-5.818
3	528	-5.845
4	517	-3.893
5	508	-4.245
6	500	-3.186
7	493	-3.626
8	488	-2.608
9	484	-3.108
10	481	-2.588
11	479	-1.041

The net radiation emitted in the transparent band of the window is

$$q_T = \sum S \Delta x q''' \quad (37)$$

where $S = 1/2$ for the surface nodes and $S = 1$ for the interior nodes. Substituting the above data into Eq. (37) and solving yields $q_T = 3.014$ watts/cm². An alternate means of calculating q_T is based on the fact that the net heat flow into the specimen is zero at thermal equilibrium. Therefore

$$q_T^* = q_1'' - q_{11}'' - (q_{\text{radiation}})_1 - (q_{\text{radiation}})_{11} \quad (38)$$

$$q_T = 3.784 - 0.15 - 0.392 - 0.235 = 3.014 \text{ watts/cm}^2$$

which checks with the first solution (based on Eq. (37)).

An average effective "transparent" emissivity, ϵ_T , can be written as a function of q_T as follows:

$$\epsilon_T = \frac{q_T}{(\sigma T^4)_1 + (\sigma T^4)_{11}} \quad (39)$$

where p is the per cent of energy emitted at temperature T in the transparent region of the window. Substituting the values of q_T , T_1 , T_{11} , P_1 and P_{11} that are obtained from the computer output into Eq. (39) yields

$$e_T = \frac{3.014}{(0.53)(0.20) + (0.29)(0.13)} = 20.9$$

which is unrealistic since emissivity by definition is bounded by 0 and 1. However, this value, which is indirectly determined by the MRD computer program, does explain the disagreement between the analytical and experimental results -- the MRD program causes the glass to radiate away much more heat than it is theoretically capable of doing and consequently the window is cooled to an equilibrium temperature that is too low. This conclusion was then verified by modifying the program to enable the q''' terms to be multiplied by a weighting coefficient, W . By using a coefficient of $W \approx 1/e_T \approx 1/20.9$ the computer results give good agreement with the experimental and empirical curves plotted in Figure 24.

Since the effective "transparent" emissivity of the computer program is too high, the rate of cooling should also be too large. This was investigated by running a transient test experimentally and on the computer in which a window was allowed to cool by radiation and natural convection from approximately 900 F to room temperature. The results, which are plotted in Figure 25, corroborate the conclusions based on the previous evaluation tests -- that the subject computer program yields q''' terms (and therefore temperatures) that are significantly in error.

The present program will not be able to correctly analyze film covered windows until the difficulties in the nonfilm program are resolved. The computer results of gold and tin oxide on aluminosilicate substrates do not agree with the experimental results, but it cannot be ascertained whether or not the disagreements are entirely due to the faulty portion of the program that is not directly related to the film theory.

However, it can be said that the two wavelength bands employed by the subject computer program are definitely inadequate to properly define the required film properties. Lis et al., of MRD approximated the apparent reflectivity of a 0.2μ gold film to be about 0.9 for all wavelengths as shown in their graph which is reproduced in Figure 26 (Ref. 16). They discussed the restrictions imposed by their limitation of two wavelength bands as follows: "It must be emphasized that, like the absorption coefficient approximations, the apparent properties for the film materials are a gross simplification to the actual data and are used as a necessary first approximation to the actual data. . . (the) gold film apparent reflectivity is poorly represented by two wavelength bands."

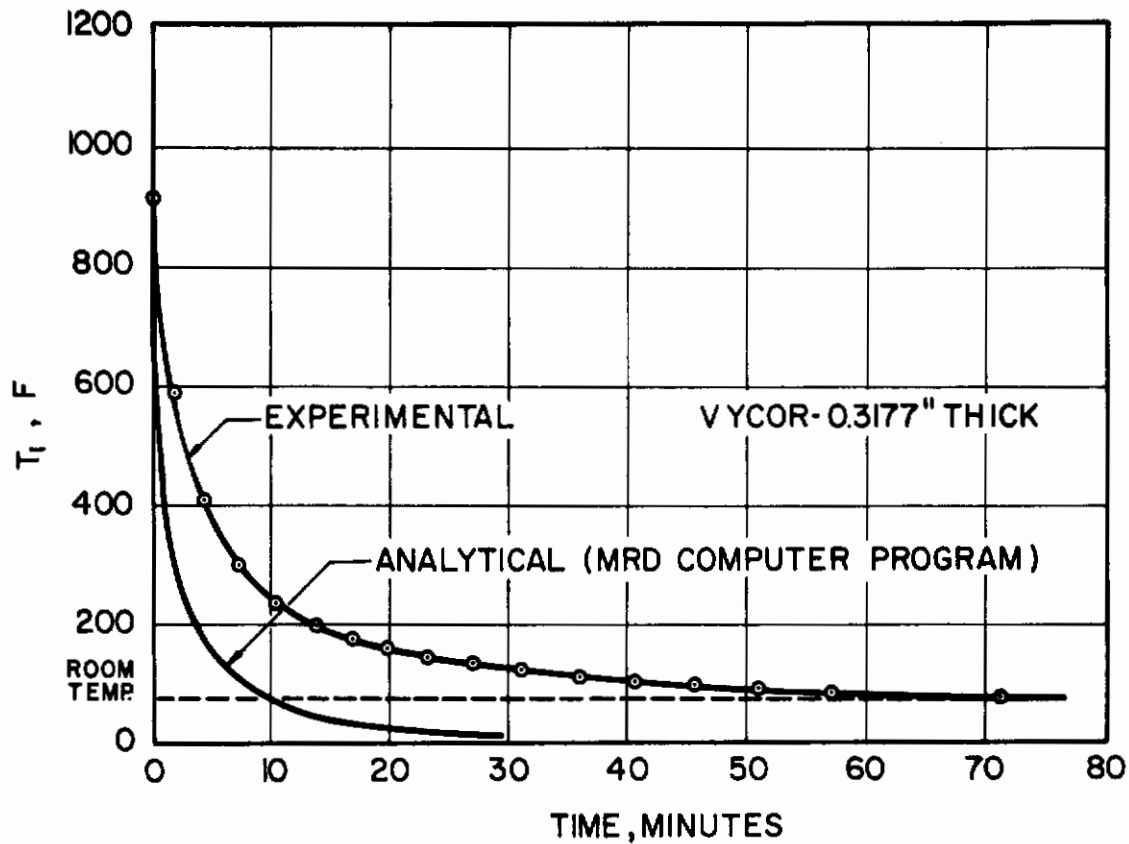


Figure 25 - Comparison of Experimental and Analytical Transient Results

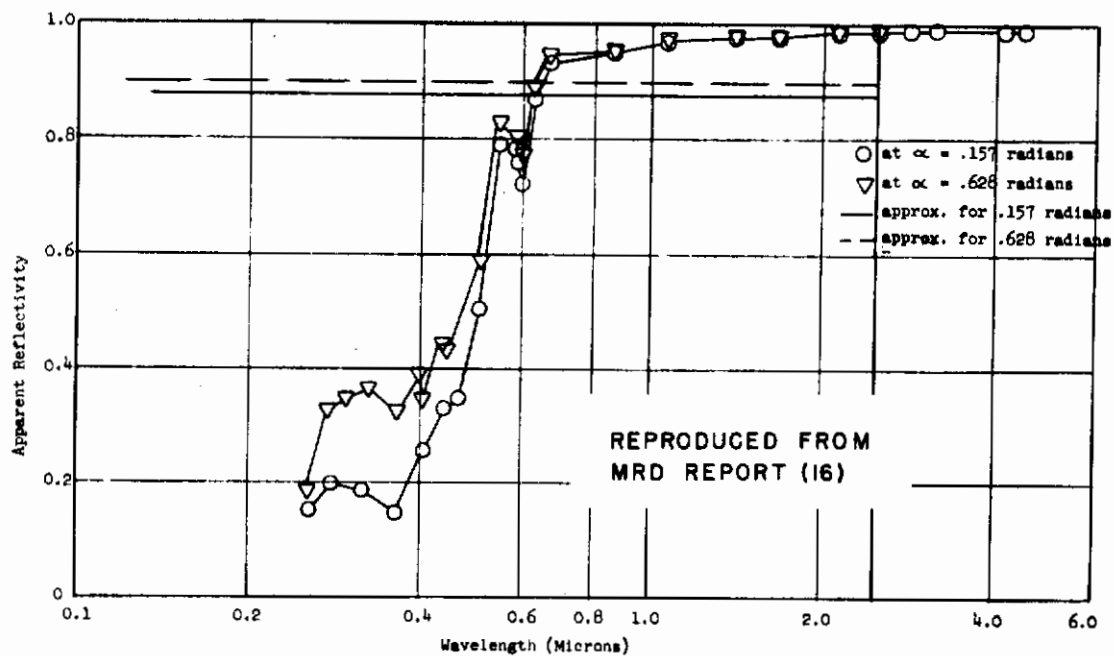


Figure 26 - First Order Approximation of Reflectance of a Thin Gold Film

The MRD first order approximation of apparent total hemispherical transmissivity of a 0.2μ gold filmed aluminosilicate glazing is about 4×10^{-5} . Both this value and the apparent reflectivity approximation (0.9) indicate that a 0.2μ gold film is opaque. If this were the case the window would be rendered useless due to a complete loss of visibility. In reality, a 0.2μ gold film is semitransparent; this is apparent from the photograph in Figure 12 and the spectral transmittance curve in Figure 13.

In view of the unrealistic film properties and the significant errors in computing the q'' terms, it is concluded that the subject program in its present form is not a satisfactory analytical tool for estimating heat fluxes and temperature distributions in diathermanous materials.

After completing the evaluation program, MRI consultant Robert Gardon (a) independently analyzed the experimental, empirical, and analytical results, (b) critiqued the MRI evaluation and procedures and conclusions, (c) briefly studied the MRD theory and (d) offered opinions and recommendations concerning the over-all project. After performing this work, Gardon judged that the MRI evaluation procedures were reasonable and in general concurred with MRI's primary and secondary conclusions.

V. CONCLUSIONS AND RECOMMENDATIONS

The MRD computer program for analyzing heat transfer to, within, and from diathermanous materials was evaluated by MRI. A primary objective of the evaluation was to determine whether the program in its present stage of development was a valid analytical tool that could be used with complete confidence. Several independent studies involving experimental, empirical, and analytical tests were conducted by MRI to answer this question. The findings of each of these investigations are in very close agreement and all lead to and support the MRI conclusion that: the subject computer program does not give realistic results and thus in its present form is not a satisfactory means of estimating heat fluxes and temperature distributions in diathermanous materials.

Secondary conclusions relative to the MRD program include:

1. An increase in the number of wavelength bands from two to five or more can significantly improve the results;
2. Data preparation is complicated, time consuming, and requires that the program user read in glass properties and Planck's blackbody spectral energy data and otherwise be unnecessarily familiar with the theoretical considerations underlying the program;
3. A faulty logic test is responsible for the discontinuous nature of q''' at nodes 9 and 11 and is most pronounced for relatively opaque diathermanous materials;
4. Opaque materials are correctly analyzed;
5. Computed values of q''' are much too large; thus, diathermanous materials are incorrectly analyzed;
6. Radiation from the cabin to the window is not accounted for in the thermal balance of node 11; and
7. The two-band limitation results in the use of unrealistic gold film properties.

Significant findings relative to the experimental program conducted by MRI include:

1. The transparent boundary apparatus, which was designed to give realistic boundary conditions, yielded good experimental data;

2. It was found that radiative and convective heaters could be designed to give a uniform heat flux across the window surface;

3. The gold temperature sensors were accurate, sensitive, stable, and had a negligible influence on the local heat flux and temperature.

Robert Gardon, who developed the basic theory employed by MRD, concurred in general with the MRI evaluation procedures and conclusions. With respect to one typical computer run he reported, "I still believe our rough overall heat balance on the glass and therefore cannot trust the computer results as they stand" (Ref. 17).

Despite the program difficulties, MRI investigators and Gardon believe that the basic theory is sound. It is also believed that if more emphasis were now placed on obtaining realistic results rather than concentrating on intricate and perhaps inconsequential theoretical details, a valid and useful program could be developed. Such a program would make an important contribution to the design of advanced systems such as the SST and the Scramjet. With the predicted heat loads for these vehicles being several times larger than those encountered by current aircraft and with radiation heat transfer in diathermanous materials increasing rapidly as a function of temperature, the lack of an accurate and reliable method for the thermal analysis of window systems could be a serious limiting factor in the design of future aerospace vehicles. Therefore, it is strongly recommended that development of this complex computer program to predict heat fluxes and temperatures in transparent materials be continued.

The progress to date has been orderly: developing the theory, writing a computer program, and evaluating the program. The next logical step is to modify the basic program to make it accurate, reliable, and applicable to actual design studies and problems. Additional refinements and versatility could be added later, but in the meantime FDL engineers could be using an operational program.

Based on our evaluation and understanding of the theory and program we recommend that the following research be initiated:

1. Conduct a thorough analysis of the computer program to further isolate the area(s) of difficulty;

2. Perform modifications to correct the above difficulties;

3. Incorporate, refine and document the following temporary changes made by MRI (see III-C);

- a. Allow the radiation interchange terms to be integrated over any number of wavelength bands;
 - b. Add an opaque short wavelength band;
 - c. Allow the material properties to be temperature dependent; and
 - d. Permanently correct the faulty test described in III-D;
4. Simplify the data input requirements. This includes the following:
 - a. Incorporate the invariable relationship between per cent of blackbody energy and the product of wavelength and temperature as part of the main program;
 - b. Store thermal and optical properties of glasses applicable to aircraft window systems in the body of the program;
 5. Add an option to allow heat flux information to be read in as data so that the user will not be restricted to trajectories and flight paths that are somewhat limited;
 6. Make the output more useful to FDL engineers. This includes improving the printed format and adding an option for plotting the results;
 7. Take into account the heat that is radiated from the cabin to the window;
 8. Evaluate the new version of the program by comparing it with MRI experimental data (Appendix C) and by conducting tests similar to those described in Section III;
 9. Write a user's manual;
 10. Work closely with the FDL engineer(s) to insure effective information transfer pertaining to the use of the program, interpretation of results, and application of the program to practical problems. This would involve a short training period after the program has been developed and verified;
 11. Reevaluate the film theory after incorporating the modifications to correct the nonfilm theory; and

12. Analyze the experimental apparatus to determine what changes would be required to run at temperatures approaching 2000 F.

Minor tasks too detailed to include in the above summary are also recommended. Major tasks that should be carried out at a later date include experimental testing at higher temperatures, correcting any existing film difficulties, expanding the experimental capabilities to include multiple glazes, and evaluating the multiglaze computer program. However, in order to obtain a useful program in the least amount of time we believe that the 12-step program outlined above should first be completed.

APPENDIX A

PROPERTIES OF DIATHERMANOUS MATERIALS

PROPERTIES OF DIATHERMANOUS MATERIALS

The following optical and thermophysical properties are employed in the theory developed by Gardon: thermal conductivity, absorption coefficient, index of refraction, the product of density and specific heat, and emissivity (for wavelength bands where the material is opaque).

Thermal conductivity values cannot be measured directly without including the effects of so-called radiative conduction; however, ingenious methods of partially eliminating radiation have been devised. For example, Flynn and Robinson (Ref. 18) determined the thermal conductivity of borosilicate by measuring the temperature gradient between two foils in contact with the specimen surfaces; external radiation was indirectly eliminated by extrapolating the results to zero emissivity. It is much more difficult, if possible at all, to experimentally eliminate internal radiation; however, for moderate temperatures this component is relatively insignificant. For high temperatures (say above 1500 F) a better means of determining true thermal conductivity will have to be developed.

The property, absorption coefficient, is related to the attenuation of intensity of a monochromatic beam of radiation over a distance x by the Bouguer-Lambert Law:

$$I_x = Ie^{-\gamma x} \quad (A-1)$$

The absorption coefficient can be developed as a function of transmittance, normal reflectance, and specimen thickness as follows. Transmittance, which is a function of thickness and thus is not a true property is expressed as

$$\tau = I_{out}/I_{in} \quad (A-2)$$

where I_{in} is the intensity of a beam entering the specimen and I_{out} is the intensity as it exits from the opposite surface. The incoming beam, which is assumed to be normal to the glass surface, is partially reflected at the first surface, is attenuated as it passes through the semitransparent medium, and is partially reflected at the second surface such that

$$I_{\text{out}} = \left\{ 1 - \rho_N \right\} \left\{ \left[(1 - \rho_N) I_{\text{in}} \right] e^{-\gamma L} \right\} \quad (\text{A-3})$$

where L is the specimen thickness. Combining Eqs. (A-2) and (A-3) yields

$$\tau = (1 - \rho_N)^2 e^{-\gamma L} \quad (\text{A-4})$$

For most glasses, hemispherical and normal reflectance are related approximately as

$$(1 - \rho_H) \cong 0.95 (1 - \rho_N) \quad (\text{A-5})$$

Substituting Eq. (A-4) into Eq. (A-5) and rearranging gives the desired relationship:

$$\gamma \cong \frac{-\ln \left[0.90 \tau / (1 - \rho_H)^2 \right]}{L} \quad (\text{A-6})$$

The other properties are readily measured and calculated.

APPENDIX B

DERIVATION OF THE LOCAL CONFIGURATION FACTOR FOR PARALLEL,
DIRECTLY OPPOSED, PLANE CIRCULAR DISKS

DERIVATION OF THE LOCAL CONFIGURATION FACTOR FOR PARALLEL, DIRECTLY OPPOSED, PLANE CIRCULAR DISKS

The net heat radiated from the window to the external heater is

$$q = F_{WH} \sigma (T_W^4 - T_H^4) \pi R_W^4 \quad (B-1)$$

where F_{WH} is the fraction of radiant energy leaving the window that is incident upon the heater. The configuration factor F_{WH} is related to F_{HW} by the basic reciprocity law

$$F_{WH} = \frac{F_{HW} A_H}{A_W} \quad (B-2)$$

The average value of F_{HW} can be obtained from equations developed by Hamilton and Morgan (Ref. 10) which are of the following form:

$$F_{HW} = 1/2 \left[\chi - (\chi^2 - 4E^2 D^2)^{1/2} \right] \quad (B-3)$$

where

$$E = \frac{R_W}{h} \quad , \quad (B-4)$$

$$D = \frac{h}{R_H} \quad , \quad \text{and}$$

$$\chi = 1 + (1 + E^2) D^2 \quad . \quad (B-6)$$

Computation of the local value of F_{HW} at r_W is illustrated in the following example: $h = 2.0$ in., $R_W = 2.0$ in., $R_H = 3.0$ in., and $r_W = 1.0$ in. First, a window disk having a radius of 1.1 in. is subdivided into a 0.9 in. radius disk and a surrounding ring. It follows that

$$(F_{HW})_{R_W=1.1} A_H = (F_{HW})_{R_W=0.9} A_H + (F_{HW})_{\text{ring}} A_H \quad (\text{B-7})$$

therefore

$$(F_{HW})_{\text{ring}} = (F_{HW})_{R_W=1.1} - (F_{HW})_{R_W=0.9} \quad (\text{B-8})$$

Solving Eq. (B-3) for $R_W = 1.1$ and 0.9 and substituting into Eq. (B-8) gives

$$(F_{HW})_{\text{ring}} = 0.090 - 0.061 = 0.029$$

The value F_{HW} is proportional to the window area being considered; the above value is with respect to the ring having radii of 1.1 in. and 0.9 in. The value of F_{HW} for the total disk based on the local conditions at $r_W = 1.0$ is

$$\text{Local } (F_{HW})_{R_W=2.0} = (F_{HW})_{\text{ring}} \times \frac{A_W}{A_{\text{ring}}} = 0.029 \times \frac{\pi (2.0)^2}{\pi [(1.1)^2 - (0.9)^2]}$$

$$\text{Local } (F_{HW})_{R_W=2.0} = 0.29$$

Substituting this value into Eq. (B-2) yields

$$\text{Local } (F_{WH}) = 0.29 \frac{\pi (3.0)^2}{\pi (2.0)^2} = 0.658$$

which coincides with the curve in Fig. 7 at $h = 2.0$ and $r_W/R_W = 0.5$.

APPENDIX C

EXPERIMENTAL DATA

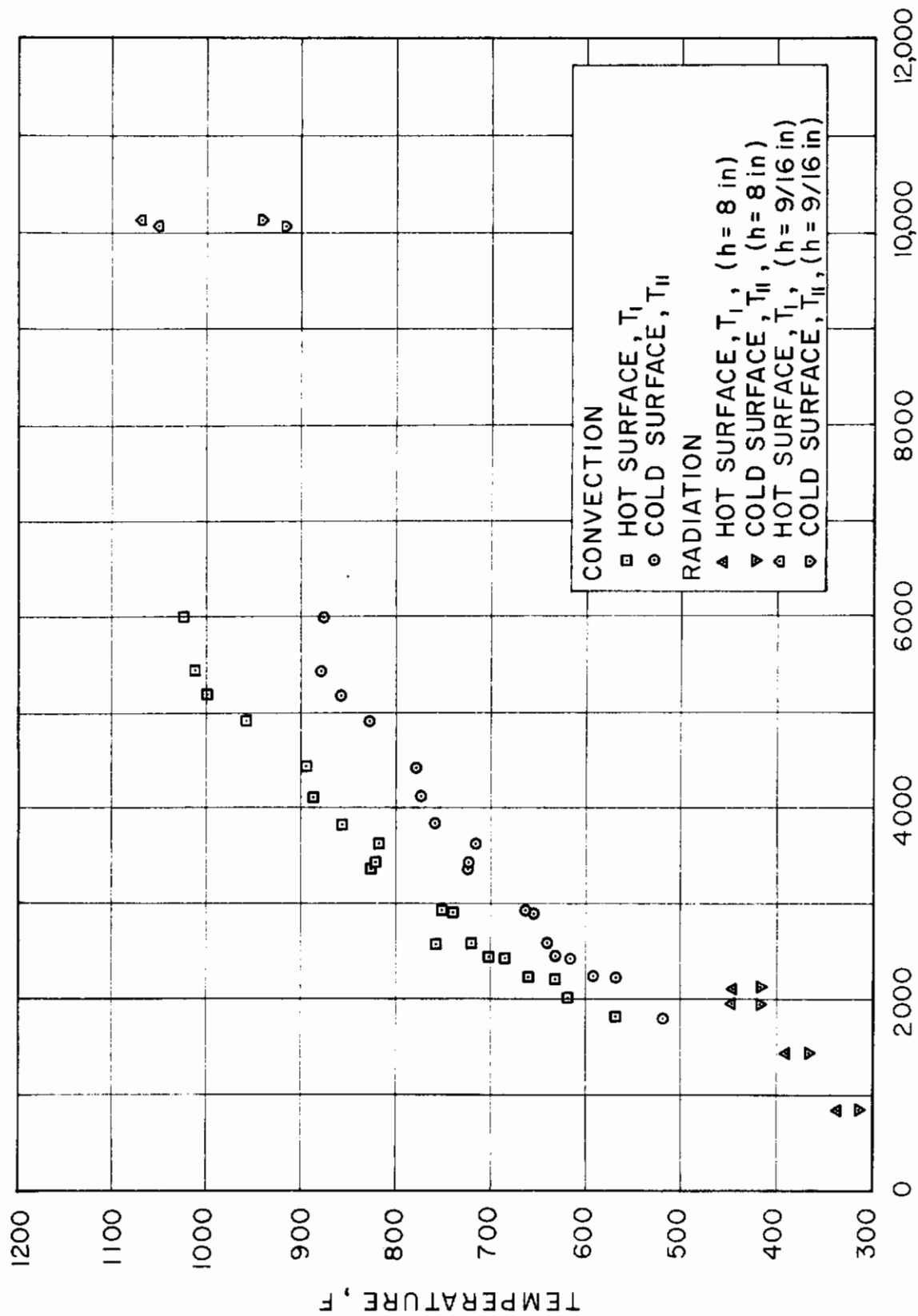


Figure C-1 - Experimental Data for 5/16 In. 96 Per Cent Silica Glass

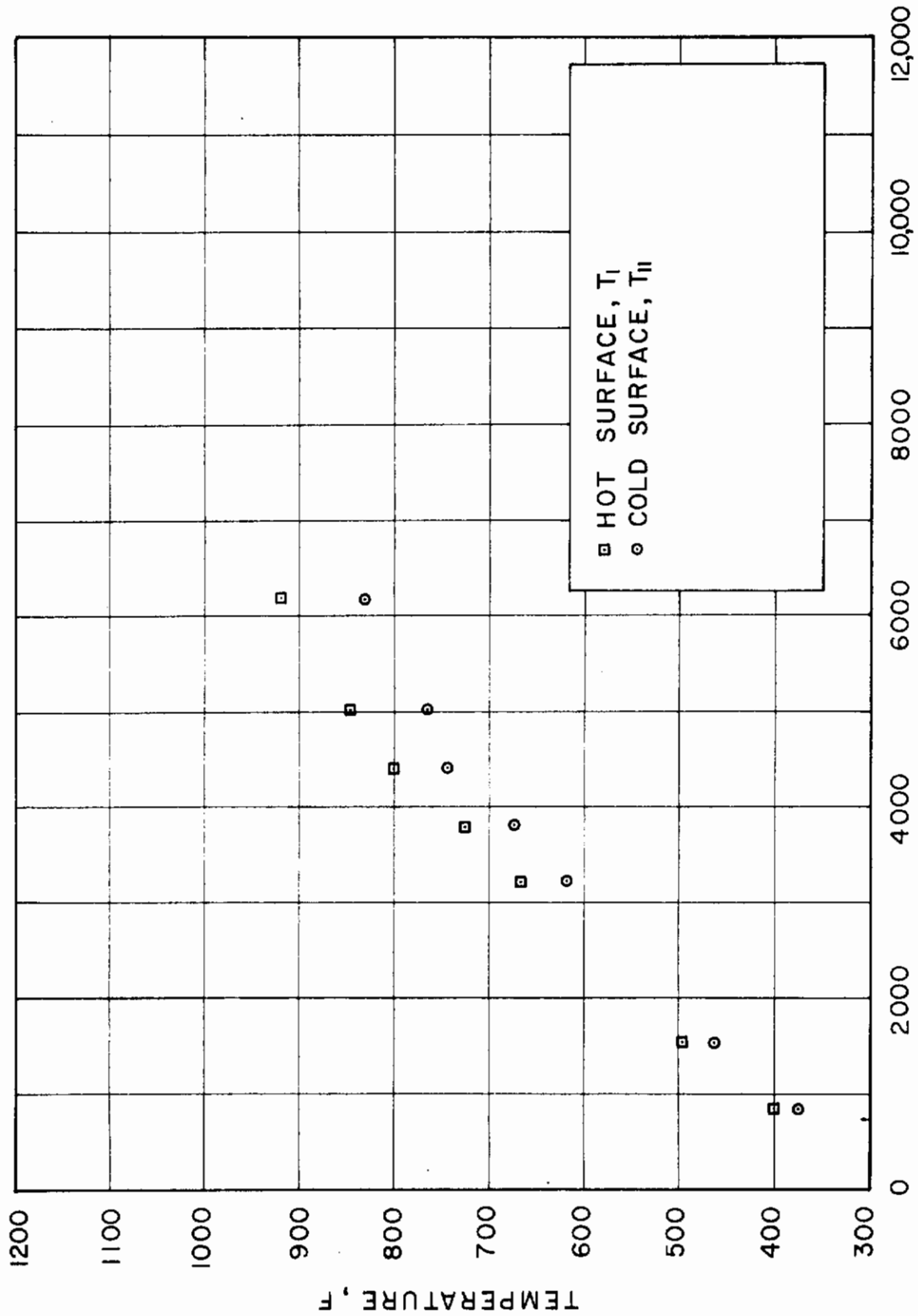


Figure C-2 - Experimental Data for 1/4 In. 96 Per Cent Silica Glass Heated by Convection

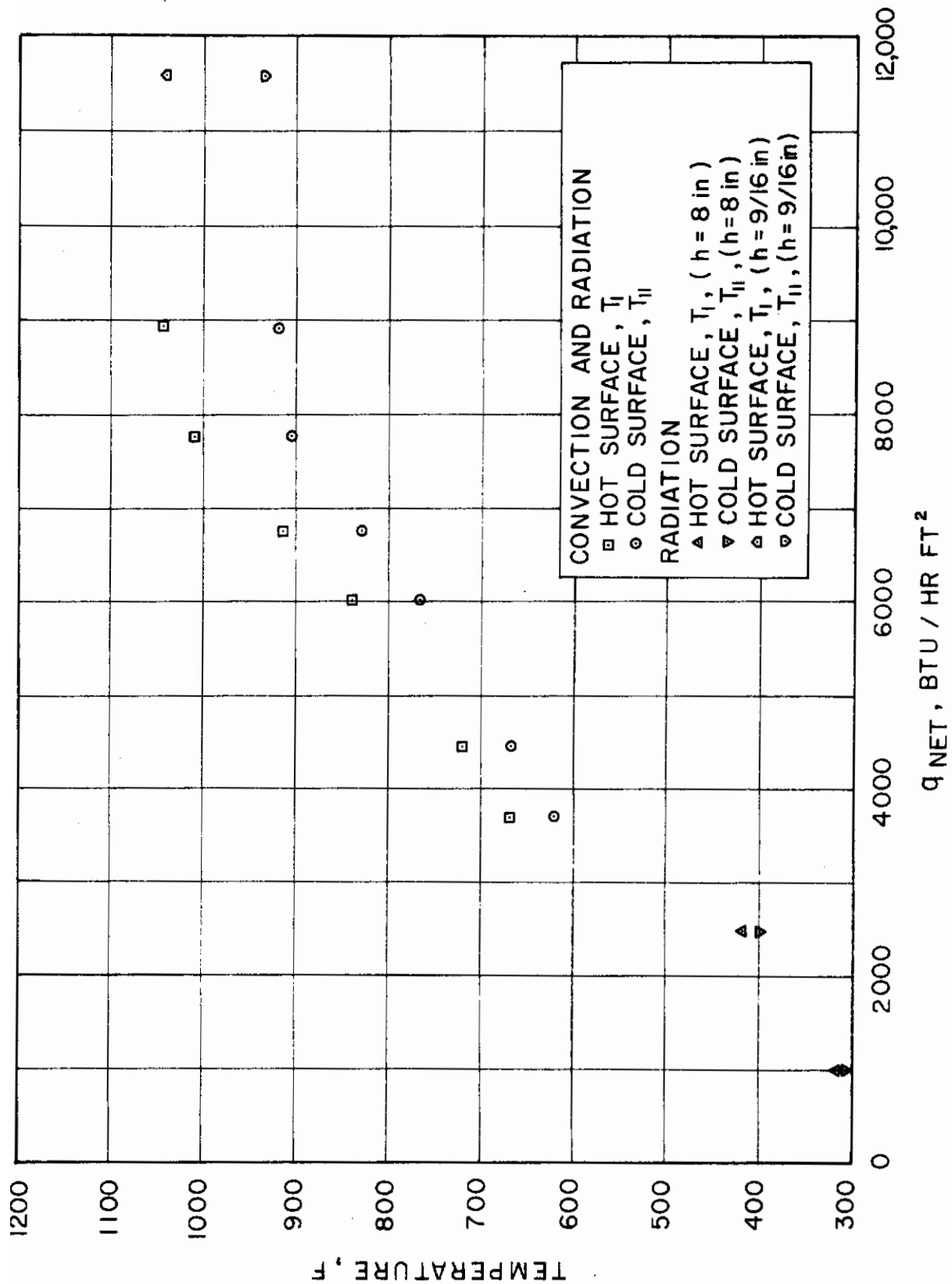
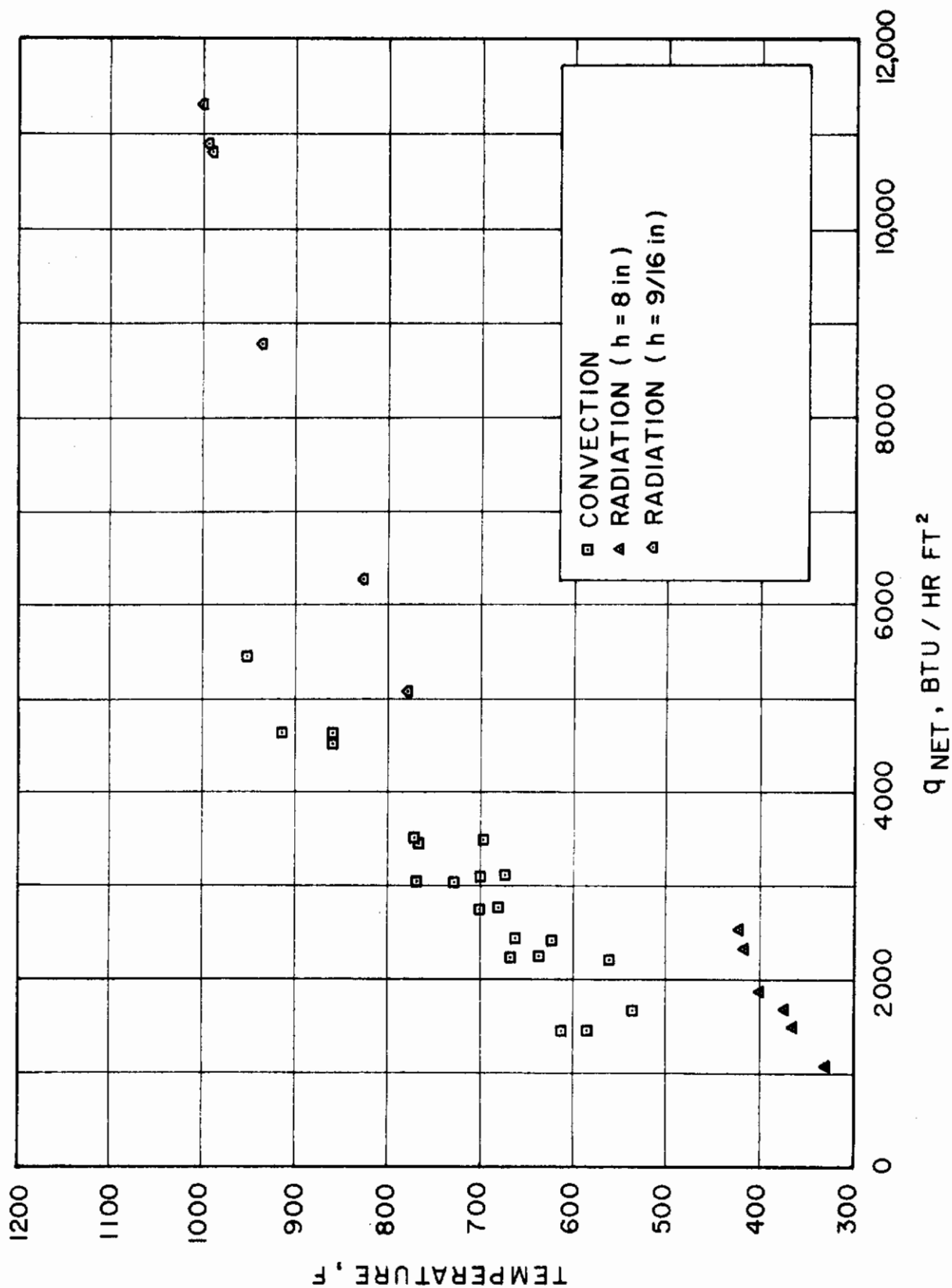


Fig. C-3 - Experimental Data for 1/4 In. 96 Per Cent Silica Glass



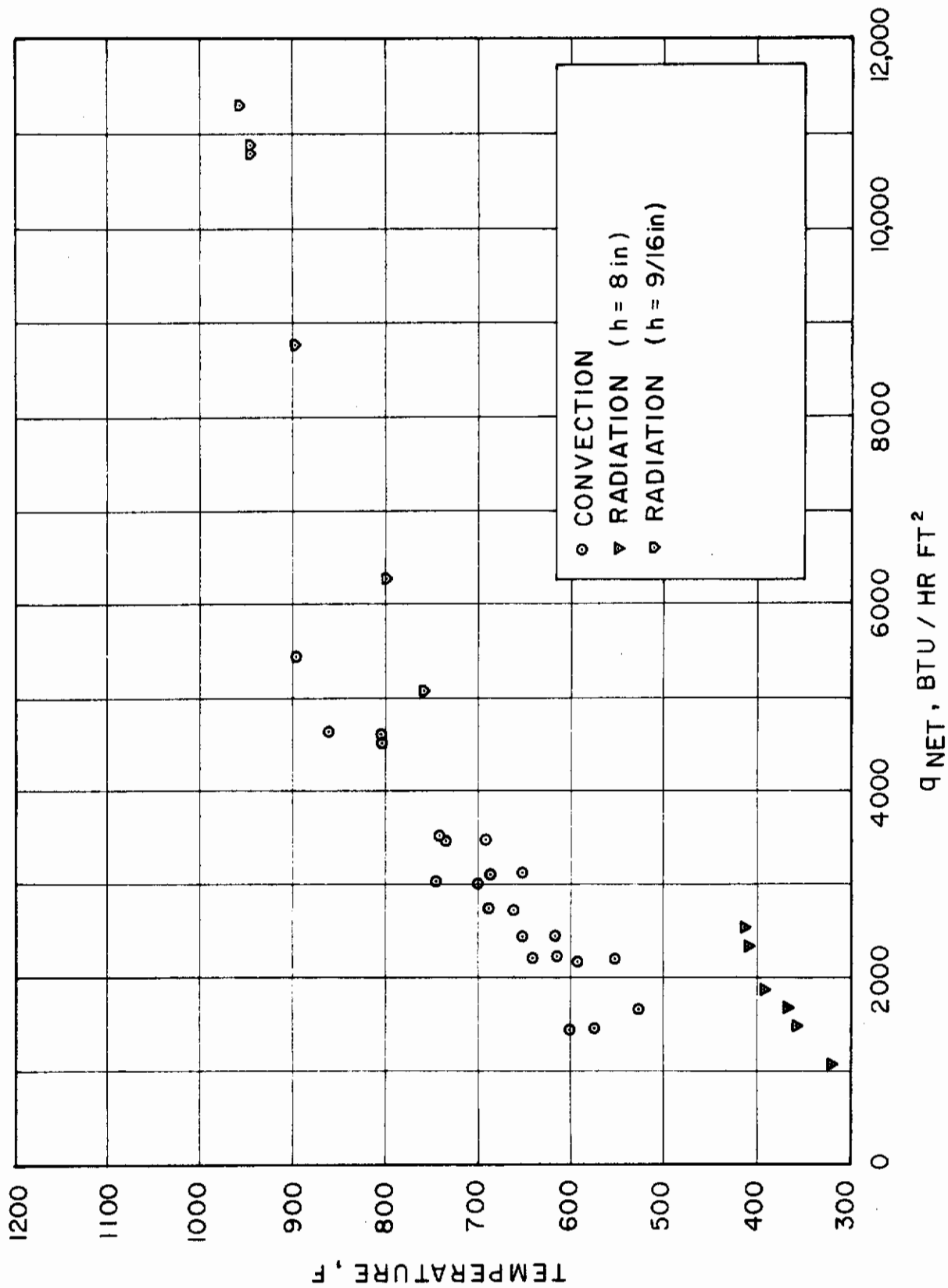


Figure C-5 - Experimental Data for 1/8 In. 96 Per Cent Silica Glass.
Recorded Temperatures are for the Cold Surface.

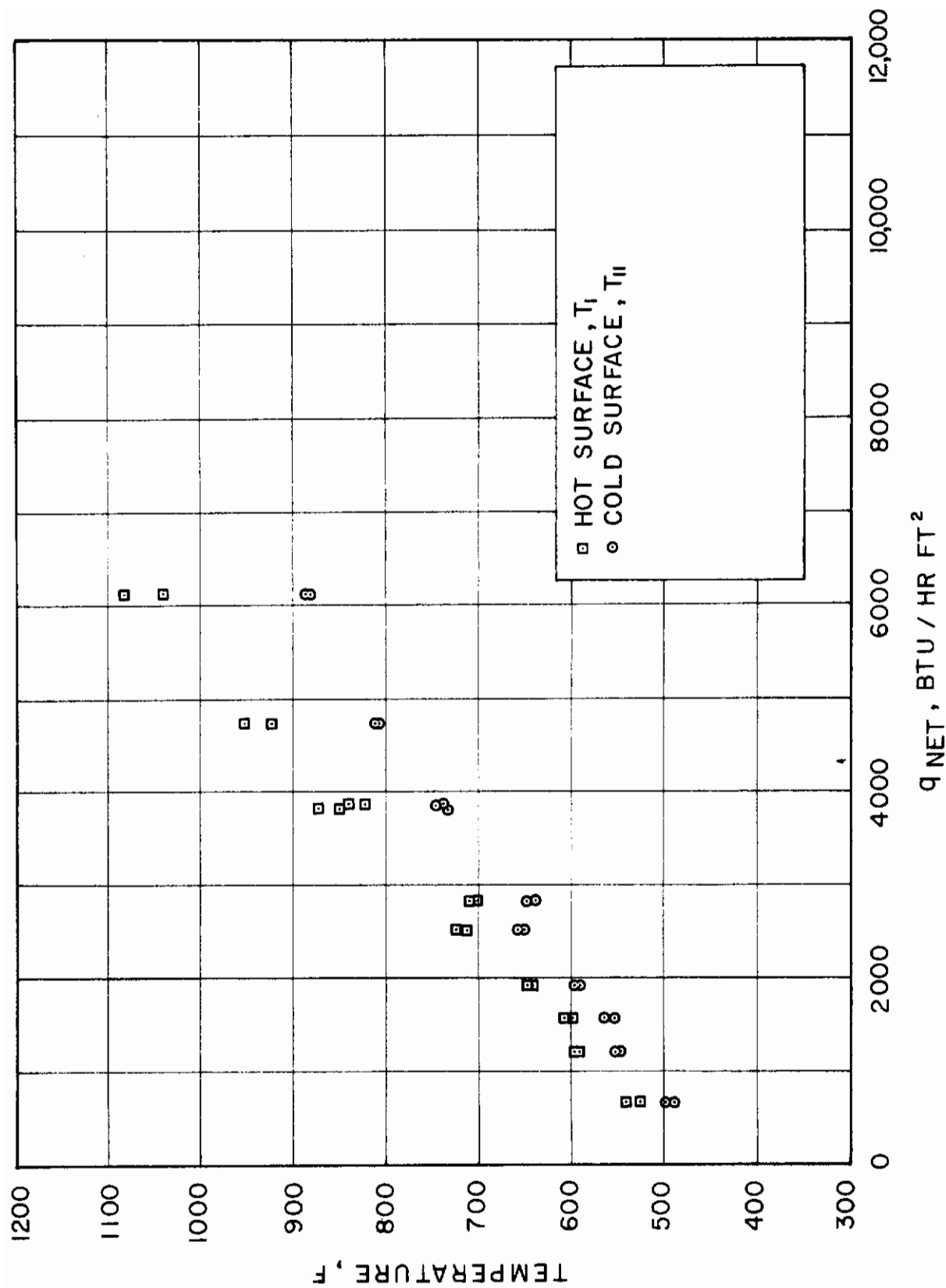


Figure C-6 - Experimental Data for 1/4 In. Aluminosilicate Glass Heated by Convection

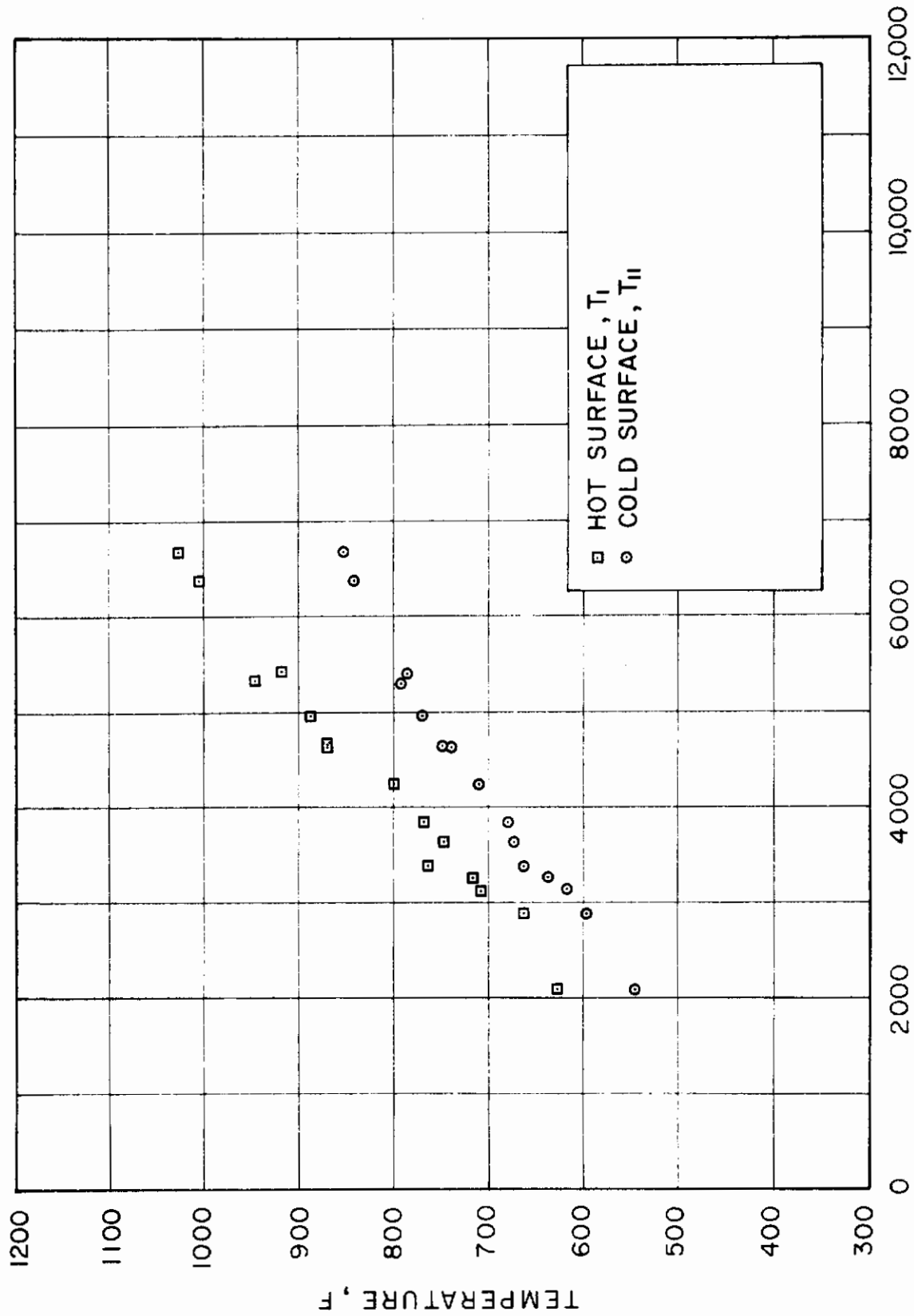


Figure C-7 - Experimental Data for 1/4 In. Aluminosilicate Glass Coated with 0.2 μ Tin Oxide Films on Both Surfaces. Specimen is Heated by Convection.

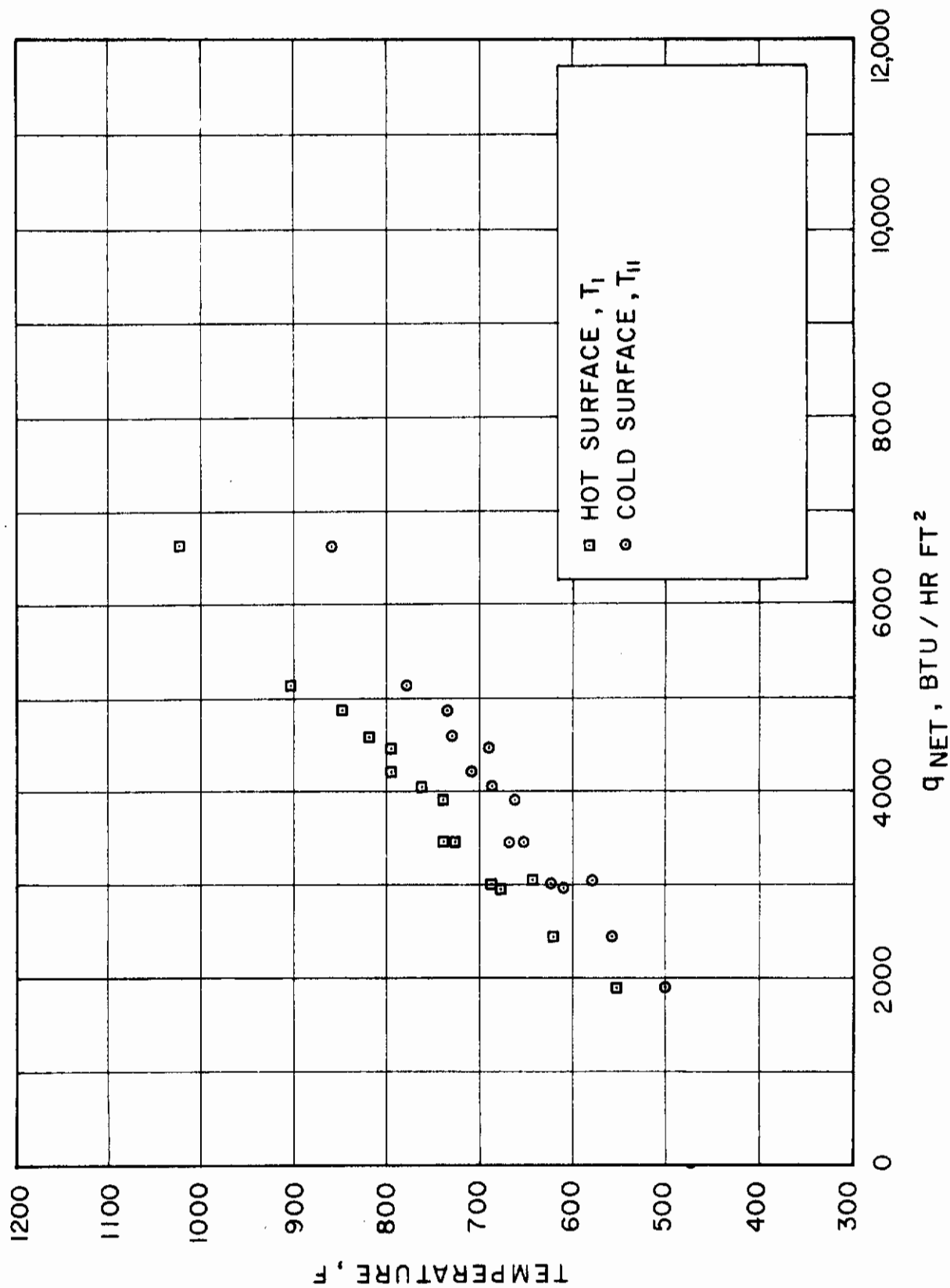


Figure C-8 - Experimental Data for 1/4 In. Aluminosilicate Glass Coated With a 0.2 μ Tin Oxide Film on the Hot Surface. Specimen Heated by Convection.

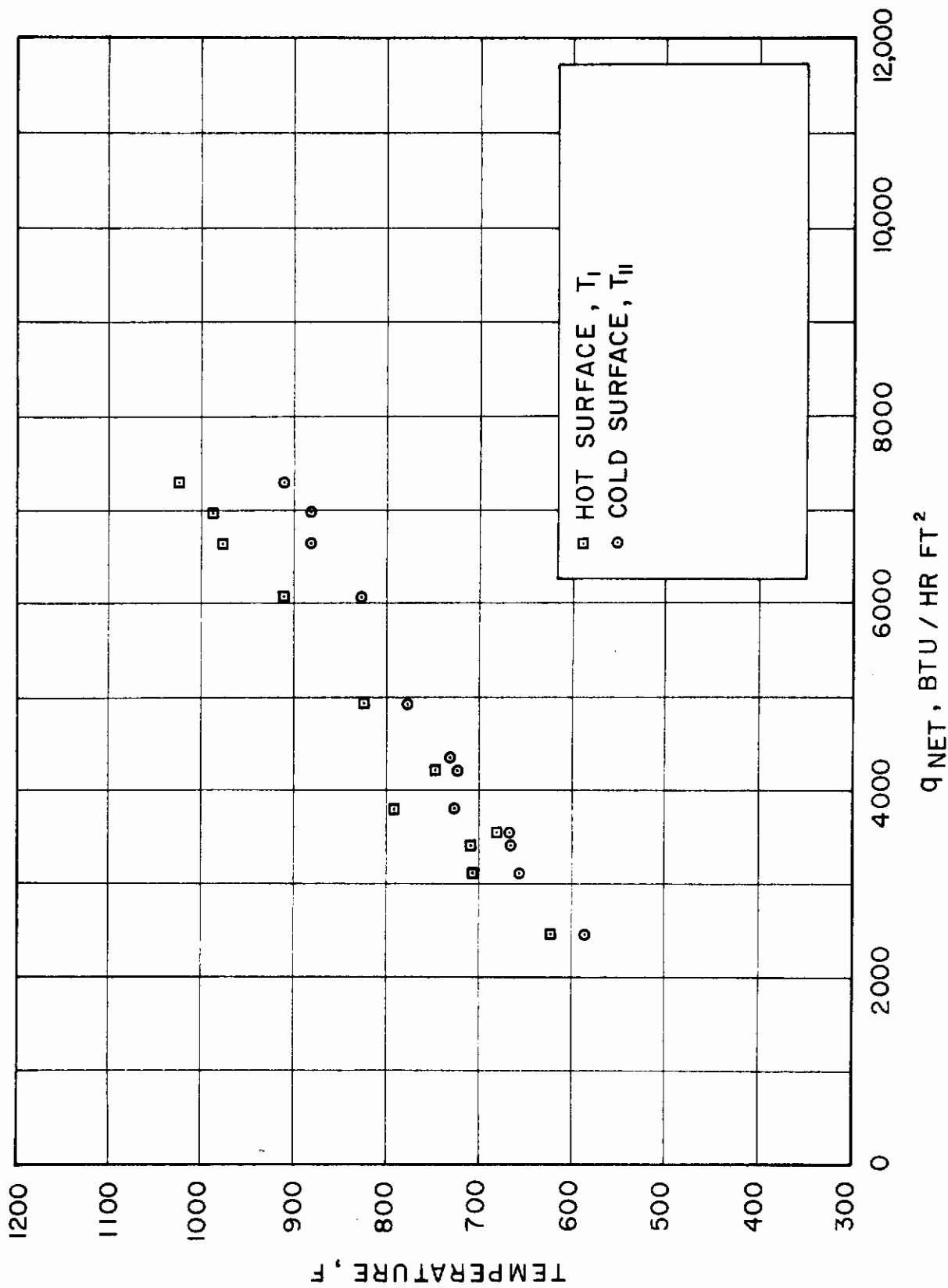


Figure C-9 - Experimental Data for 1/4 In. Aluminosilicate Glass Coated With a 0.2 μ Tin Oxide Film on the Cold Surface. Specimen Heated by Convection.

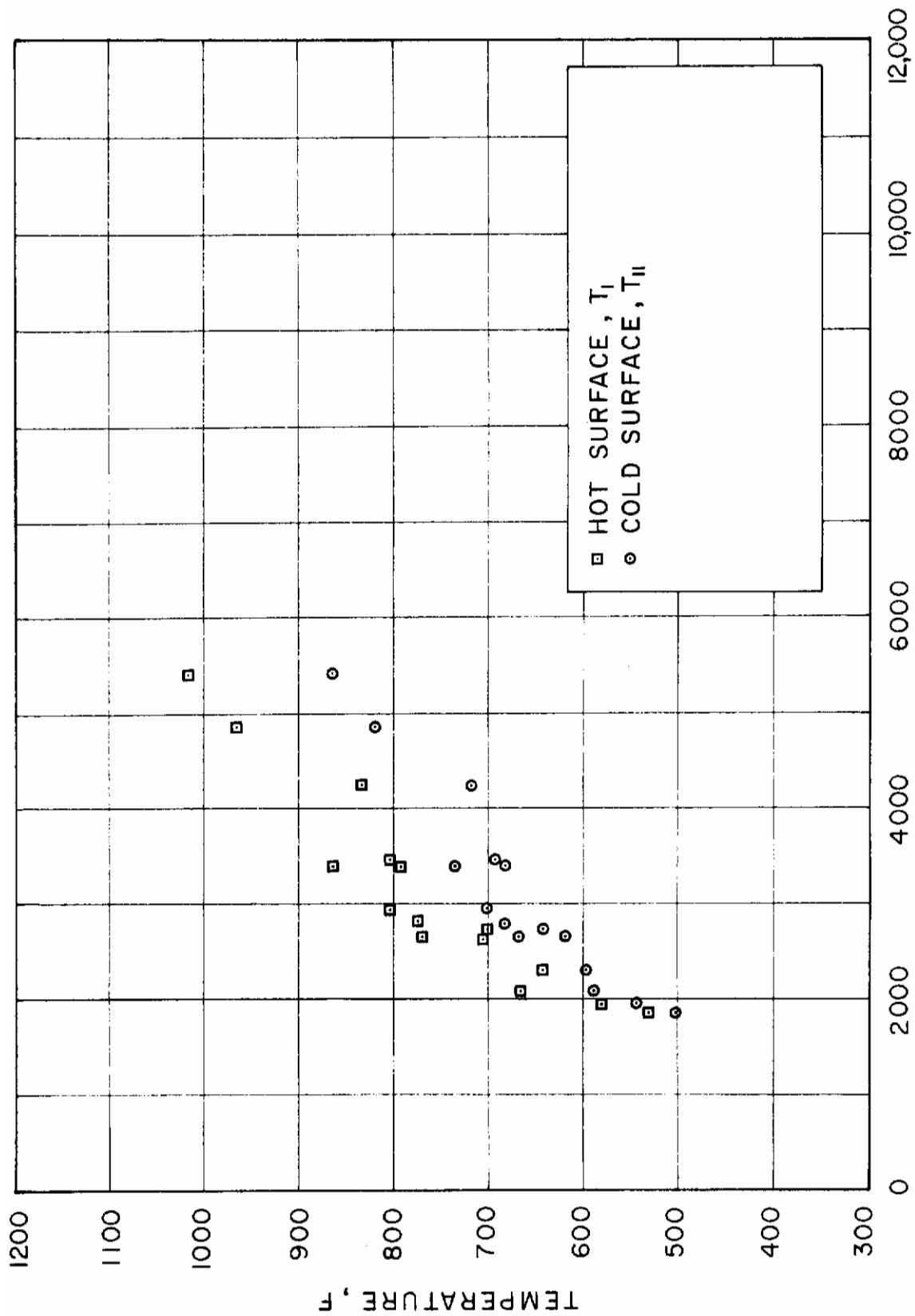


Figure C-10 - Experimental Data for 1/4 In. Aluminosilicate Glass Coated with 0.2 μ gold Films on Both Surfaces. Specimen Heated by Convection.

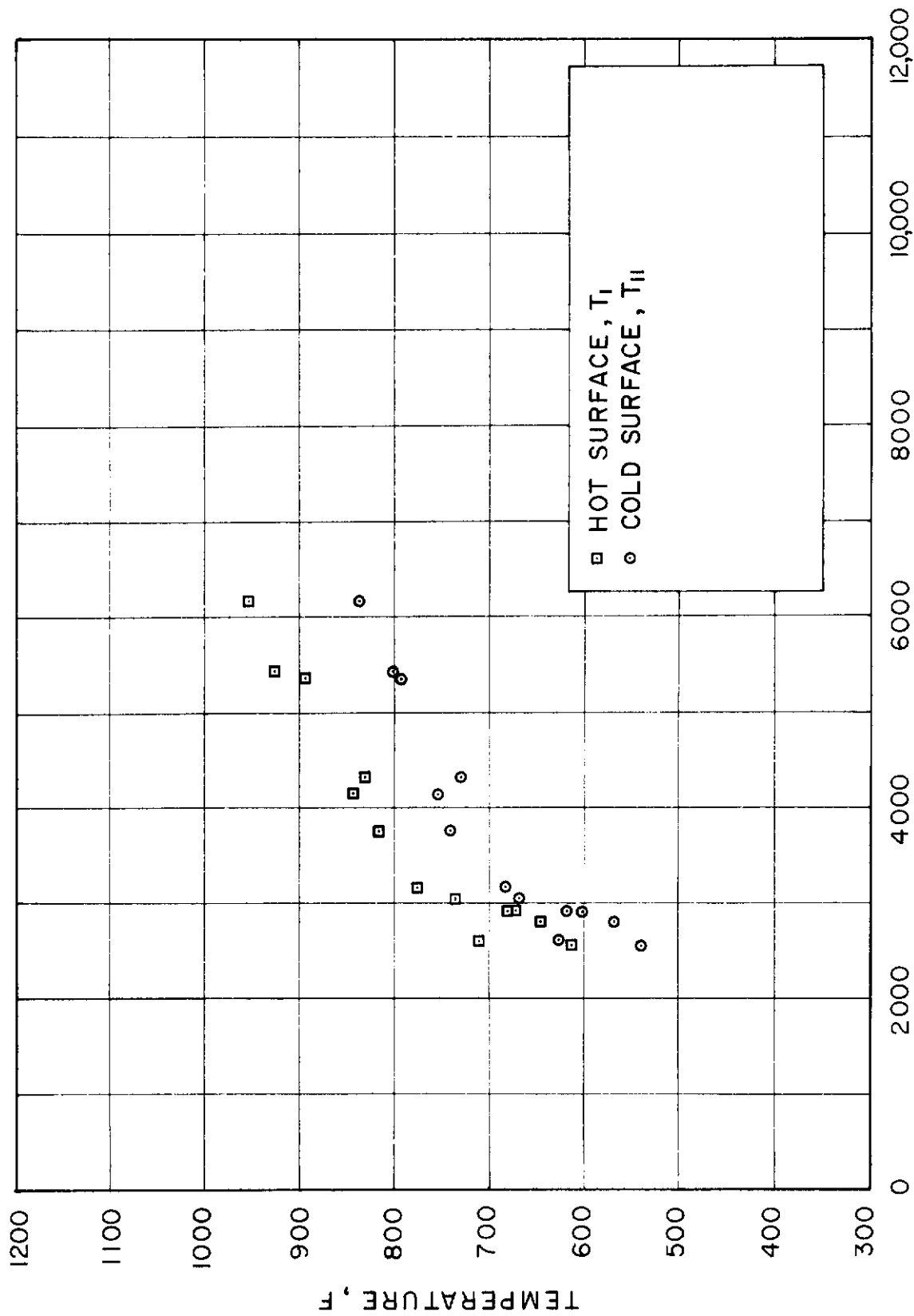


Figure C-11 - Experimental Data for 1/4 In. Aluminosilicate Glass Coated With a 0.2μ Gold Film on the Cold Surface. Specimen Heated by Convection.

REFERENCES

1. Kingery, W. D., "Thermal Conductivity: WIV, Conductivity of Multicomponent Systems," J. Am. Cer. Soc., 42, 617-627 (1959).
2. Lee, D. W., and W. D. Kingery, "Radiation Energy Transfer and Thermal Conductivity of Ceramic Oxides," J. Am. Cer. Soc., 43, 594-607 (1960).
3. Gardon, Robert, "Emissivity of Transparent Materials," J. Am. Cer. Soc., 39 (1956).
4. Gardon, Robert, "A Review of Radiant Heat Transfer in Glass," J. Am. Cer. Soc., 44, 305-312 (1961).
5. Flynn, D. R., and H. E. Robinson, "Thermal Conductivity of Semiconductive Solids; Method for Steady-State Measurements on Small Disc Reference Samples," National Bureau of Standards Report No. 7135 (1961).
6. Kreith, Frank, Radiation Heat Transfer, International Textbook Company, Scranton, Pennsylvania, 1962, p. 11.
7. Hottel, H. C., "Radiat Heat Transmission," Chapter 4 in W. B. McAdams' Heat Transmission, McGraw-Hill Book Company, Inc., New York (1954).
8. Eckert, E. R. G., and R. Drake, Heat and Mass Transfer, McGraw-Hill Book Company, Inc., New York, 1959.
9. Op. cit., Chapter 3 and Appendix V.
10. Hamilton, D. C., and W. R. Morgan, "Radiant Interchange Configuration Factors," NACA TN2836 (1952).
11. Gardon, Robert, and John Cobonpue, "Heat Transfer Between a Flat Plate and Jets of Air Impinging on It," International Development, in Heat Transfer, Part II, Proceedings of 1961 International Heat Transfer Conference, ASME, New York, 1961.
12. Deverall, J. E., "The Thermal Conductivity of a Molten Pu-Fe Eutectic," USAEC Report LA-2269, 1-62 (1959).
13. Przybycien, W. M., and D. W. Linde, "Thermal Conductivities of Gases, Metals, and Liquid Metals," USAEC Report KAPL-M WWP-1, 1-24 (1957).

REFERENCES (Concluded)

14. Ewing, C. T., R. E. Seebold, J. A. Grand, and R. R. Miller, "Thermal Conductivity of Mercury and Two Sodium-Potassium Alloys," J. Phys. Chem., 59, 524-528 (1955).
15. Gardon, Robert, "Calculation of Temperature Distributions in Glass Plates Undergoing Heat Treatment," J. Am. Cer. Soc., 41 (1958).
16. Lis, S. J., R. G. Barile, and G. Engholm, "Window Systems for Advanced Vehicles," FDL-TDR-64-39, December, 1964.
17. Gardon, Robert, personal correspondence, May 25, 1965.
18. Flynn, D. R. and H. E. Robinson, "Thermal Conductivity of Semi-Conductive Solids; Method for Steady-State Measurements on Small Disc Reference Samples," NBS Report 7135, National Bureau of Standards, 1961.

UNCLASSIFIED

Security Classification

DOCUMENT CONTROL DATA - R&D

(Security classification of title, body of abstract and indexing annotation must be entered when the overall report is classified)

1. ORIGINATING ACTIVITY (Corporate author) Midwest Research Institute 425 Volker Boulevard Kansas City, Missouri 64110		2a. REPORT SECURITY CLASSIFICATION Unclassified	
		2b. GROUP	
3. REPORT TITLE Experimental Verification of the Analysis and Computer Programs Concerning Heat Transfer Through Semitransparent Materials			
4. DESCRIPTIVE NOTES (Type of report and inclusive dates) Preliminary Draft of Final Technical Report 1 April 1964 to 19 August 1965			
5. AUTHOR(S) (Last name, first name, initial) Finch, Harold Moeller, C. E. Noland, M.			
6. REPORT DATE June 1965		7a. TOTAL NO. OF PAGES 83	7b. NO. OF REFS 18
8a. CONTRACT OR GRANT NO. AF 33(615)-1801		9a. ORIGINATOR'S REPORT NUMBER(S) N/A	
b. PROJECT NO. 1368			
c. Task No. 136802		9b. OTHER REPORT NO(S) (Any other numbers that may be assigned this report) AFFDL-TR-65-136	
d.			
10. AVAILABILITY/LIMITATION NOTICES DDC release to the Clearinghouse for Federal Scientific and Technical Information (formerly OTS) is not authorized.			
11. SUPPLEMENTARY NOTES N/A		12. SPONSORING MILITARY ACTIVITY Structures Division Design Concepts - FDTS AFFDL - Wright-Patterson AFB, Ohio	
13. ABSTRACT An experimental and analytical evaluation of the theory and computer programs concerning heat transfer through semitransparent materials which was developed under Contract AF 33(657)-9138 by the MRD Division of the General American Transportation Corporation (MRD). Experimental investigations of the heat transfer through 96 percent silica glass and aluminosilicate glass were conducted for glaze temperatures to 1000°F. Similar data were produced for the same materials with tin oxide or gold films on one or both sides of the specimens. The experimental, empirical, and analytical tests conducted to evaluate the computer program led to the MRI conclusion that the program in its present form does not yield realistic results and thus is not a satisfactory tool for the computation of heat fluxes or temperature distributions in semitransparent materials. Recommendations for future research are based upon a belief that the theory is sound and that, despite the MRD computer program difficulties, the program can be made into an important tool for the design of advanced systems.			

DD FORM 1473
1 JAN 64

UNCLASSIFIED

Security Classification

Approved for Public Release

UNCLASSIFIED

Security Classification

Contrails

14 KEY WORDS	LINK A		LINK B		LINK C	
	ROLE	WT	ROLE	WT	ROLE	WT
Experimental Verification Heat Transfer Semitransparent Materials						

INSTRUCTIONS

1. **ORIGINATING ACTIVITY:** Enter the name and address of the contractor, subcontractor, grantee, Department of Defense activity or other organization (*corporate author*) issuing the report.

2a. **REPORT SECURITY CLASSIFICATION:** Enter the overall security classification of the report. Indicate whether "Restricted Data" is included. Marking is to be in accordance with appropriate security regulations.

2b. **GROUP:** Automatic downgrading is specified in DoD Directive 5200.10 and Armed Forces Industrial Manual. Enter the group number. Also, when applicable, show that optional markings have been used for Group 3 and Group 4 as authorized.

3. **REPORT TITLE:** Enter the complete report title in all capital letters. Titles in all cases should be unclassified. If a meaningful title cannot be selected without classification, show title classification in all capitals in parenthesis immediately following the title.

4. **DESCRIPTIVE NOTES:** If appropriate, enter the type of report, e.g., interim, progress, summary, annual, or final. Give the inclusive dates when a specific reporting period is covered.

5. **AUTHOR(S):** Enter the name(s) of author(s) as shown on or in the report. Enter last name, first name, middle initial. If military, show rank and branch of service. The name of the principal author is an absolute minimum requirement.

6. **REPORT DATE:** Enter the date of the report as day, month, year, or month, year. If more than one date appears on the report, use date of publication.

7a. **TOTAL NUMBER OF PAGES:** The total page count should follow normal pagination procedures, i.e., enter the number of pages containing information.

7b. **NUMBER OF REFERENCES:** Enter the total number of references cited in the report.

8a. **CONTRACT OR GRANT NUMBER:** If appropriate, enter the applicable number of the contract or grant under which the report was written.

8b, 8c, & 8d. **PROJECT NUMBER:** Enter the appropriate military department identification, such as project number, subproject number, system numbers, task number, etc.

9a. **ORIGINATOR'S REPORT NUMBER(S):** Enter the official report number by which the document will be identified and controlled by the originating activity. This number must be unique to this report.

9b. **OTHER REPORT NUMBER(S):** If the report has been assigned any other report numbers (*either by the originator or by the sponsor*), also enter this number(s).

10. **AVAILABILITY/LIMITATION NOTICES:** Enter any limitations on further dissemination of the report, other than those

imposed by security classification, using standard statements such as:

- (1) "Qualified requesters may obtain copies of this report from DDC."
- (2) "Foreign announcement and dissemination of this report by DDC is not authorized."
- (3) "U. S. Government agencies may obtain copies of this report directly from DDC. Other qualified DDC users shall request through _____."
- (4) "U. S. military agencies may obtain copies of this report directly from DDC. Other qualified users shall request through _____."
- (5) "All distribution of this report is controlled. Qualified DDC users shall request through _____."

If the report has been furnished to the Office of Technical Services, Department of Commerce, for sale to the public, indicate this fact and enter the price, if known.

11. **SUPPLEMENTARY NOTES:** Use for additional explanatory notes.

12. **SPONSORING MILITARY ACTIVITY:** Enter the name of the departmental project office or laboratory sponsoring (*paying for*) the research and development. Include address.

13. **ABSTRACT:** Enter an abstract giving a brief and factual summary of the document indicative of the report, even though it may also appear elsewhere in the body of the technical report. If additional space is required, a continuation sheet shall be attached.

It is highly desirable that the abstract of classified reports be unclassified. Each paragraph of the abstract shall end with an indication of the military security classification of the information in the paragraph, represented as (TS), (S), (C), or (U).

There is no limitation on the length of the abstract. However, the suggested length is from 150 to 225 words.

14. **KEY WORDS:** Key words are technically meaningful terms or short phrases that characterize a report and may be used as index entries for cataloging the report. Key words must be selected so that no security classification is required. Identifiers, such as equipment model designation, trade name, military project code name, geographic location, may be used as key words but will be followed by an indication of technical context. The assignment of links, rules, and weights is optional.

UNCLASSIFIED

Security Classification